DOI 10.5281/zenodo.18427072

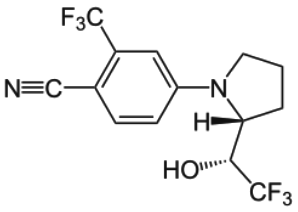

Modeling Nonlinear Pharmacokinetics: Clinical v. Anecdotal Data (LGD-4033)

Why Dosage Is Not the Same as Exposure!

Nathaniel Coulter[1*]

$\alpha\beta$stract

Can I ask you a question? Do you recall the last time you received a prescription? Whether you take medication daily for a diagnosis or were simply recovering from illness. Regardless of the dosage, did you ever consider how long the medication would remain active in your bloodstream? When would it peak, or when it would start waring off? As someone who takes ADHD medication every day, I'm fairly confident that most of us are (on some level) conscious of how long our medication is acting at maximum effectiveness. Yet, the ability to detect a medication physiologically is far less common in the majority of prescribed substances.

Recently, these questions led me to quantifying the effects of compound half-life and time decay in the bloodstream. Why is this important? Consider a scenario in which you are instructed to take a prescription once daily, the half-life is 24-36 hours, and it remains at relatively stable levels in the bloodstream during that period. If you take (say 1 mg) on day one; then on day two (24 hours later) when you take another 1 mg, the levels in your blood are higher than your prescribed dosage. As I will show, given a range of 24 to 36 hours as our half-life equates to an effective dose of 2.0x 1 mg at 24 hours and 2.7x 1 mg at a 36-hour half-life.

Although the difference between 1 mg and 2 mg may seem negligible, the accumulation factor (Linear Kinetics) DOES NOT change depending on dose. Simply put, **the 2.0x to 2.7x multiples would effectively make a dose of 10mg into a 20mg to 27mg dose when the compound has a 24-to-36-hour half-life** (in medications where concentration levels remain stable in the bloodstream during that time). In reality, the level of a medication varies between 24-36 hours depending on the speed of an individuals metabolic processes. As a result, we do address peak-trough volatility in our non-linear accumulation model.

*Department of Mathematics and Computer Science, St. John's University, NY
https://github.com/Nathaniel-Coulter/Pharmacokinetics

Contents

1 Objectives & Outline:

My only goal initially was explaining accumulation to educate the non-academic reader on the topic of *pharmacokinetics*[1]. That remains my goal. However, this research varies from a mere explanation in it's application to a community where clinical studies do not exist.

1.1 What is LGD-4033?

LGD-4033 or Ligandrol is a Selective Androgen Receptor Modulator (SARM) developed for the treatment of muscle atrophy. A SARM or Selective Androgen Receptor Modulator is a class of drug that selectively activates androgen receptors in specific tissues to promote muscle growth whilst minimizing effects on other tissues like the prostate.

1.2 Why I Chose LGD-4033 for this Report:

LGD-4033 is commonly taken by recreational bodybuilders on behalf of tissue selectively and lack of Methylation on the C7 Alkaline. The latter resulting in SARMS generally being considered far less hepatoxic (harms liver) when compared traditional anabolic steroids. Unlike traditional anabolic steroids however, LGD-4033 has not been approved for clinical studies at "effective" dosages taken by individuals. Yet, usage of these substances is far more common than traditional steroids in younger males since SARMS are legally sold as research chemicals. However, despite SARMS being less harmful in some ways—many perceive their effects on sex hormones such as Testosterone, Estrogen, and DHT to be less suppressive than traditional anabolics. This is simply not the case, but without true clinical trials quantifying their levels of suppression at given dosages, many are unaware.

2 Clinical Baseline and Model Architecture

2.1 Clinical Baseline: Basaria et al.

To anchor all subsequent analysis to medically observed outcomes, we first construct a clinical baseline using the most widely cited human trial of LGD-4033 (Basaria et al.)[1][2]. In this randomized, placebo-controlled study, healthy male subjects were administered 0.1, 0.3, or 1.0 mg/day of LGD-4033 over a 21-day period, with total testosterone measured at baseline and day 21.

[1]Pharmacokinetics (PK): is the study of how the body absorbs, distributes, metabolizes, and excretes a specific substance after administration.

Rather than treating dose as a linear proxy for exposure, we adopt the pharmacokinetic framing used in the original study and characterize exposure using the area under the concentration–time curve $AUC_{0\text{-}24,36}$. This choice captures non-linear accumulation arising from the compound's long elimination half-life and directly reflects systemic androgen receptor engagement.

For each dose level, the reported day-21 AUC and corresponding mean change in total testosterone define empirical exposure–suppression anchor points. These anchors form the sole clinical constraints imposed on the model; no extrapolation beyond observed endpoints is assumed at this stage.

2.2 Model Architecture: PK–PD Mapping with Lag and Uncertainty

Using the clinical anchors defined above, we construct a descriptive pharmacokinetic–pharmacodynamic (PK–PD) framework linking LGD-4033 exposure to testosterone suppression. Exposure is represented as a time-dependent series proportional to daily AUC accumulation, while suppression is modeled through a saturating, nonlinear response function to reflect diminishing marginal effects at higher exposure levels.

Because testosterone suppression is not instantaneous, we introduce an indirect-response (lag) dynamic that governs the evolution of testosterone over time. This structure allows suppression trajectories to emerge gradually while remaining constrained to the observed day-21 clinical endpoints.

To account for inter-individual variability in recovery dynamics, the recovery parameter α is treated as a continuous random variable. Specifically, we sample recovery half-lives H from a lognormal distribution and re-fit the suppression scaling parameter β for each Monte Carlo draw such that the model exactly reproduces the Basaria day-21 suppression at each dose. This procedure yields a family of admissible suppression trajectories rather than a single deterministic path.

Lastly, to highlight departures from linear dose assumptions at non-clinical exposure levels, we introduce a suppression velocity metric defined as the rate of percentage testosterone loss per unit time. Applied to anecdotal pre/post laboratory reports, this representation reveals regimes of rapid suppression that are not apparent when considering raw dose or endpoint suppression alone.

3 Why Your Dosages are Wrong

3.1 Linear Kinetics

When a drug is dosed at a fixed-interval, it accumulates until the amount eliminated between doses equates to the amount added. In practice, this plateau is called steady-state and it's governed by:

1. Elimination half-life
2. Dosing Interval (t)
3. Linear vs. Nonlinear clearence *(we're assuming linear for now)*

For Linear Pharmacokinetics[2], the accumulation factor is:

$$R = \frac{1}{1 - e^{-k\tau}}, \qquad \text{where} \qquad k = \frac{\ln 2}{t_{1/2}}.$$

- $t_{1/2}$ = elimination half-life
- τ = dosing interval (24 h here)

Applying to LGD-4033: (24–36 half-life)

Case 1: half-life ≈ 24 h

- $k = \ln 2/24$
- $e^{-k\tau} = e^{-0.693} = 0.5$

$e^{-0.693}$ comes from $e^{-(\ln 2/24)\times 24} = e^{-\ln 2} = 0.5$.

$$R = \frac{1}{1 - 0.5} = 2.0$$

Steady-state average ≈ 2.0× a single dose.

Case 2: half-life ≈ 36 h

- $k = \ln 2/36$
- $e^{-k\tau} \approx e^{-0.462} \approx 0.63$

$e^{-0.462}$ comes from $e^{-(\ln 2/36)\times 24} = e^{-(2/3)\ln 2} \approx 0.63$.

$$R = \frac{1}{1 - 0.63} \approx 2.7$$

Steady-state average ≈ 2.7× a single dose.

[2]Linear = rate of elimination is proportional to the amount of drug present. Dosage increases result in proportional increase in plasma drug levels.

3.2 Potential Deviations:

As stated earlier, the true half-life per individual will lie somewhere inbetween 24-36 hours. In the case of LGD-4033 specifically—where blood levels are privy to less daily oscillation according to research[3] centered on metabolite detection for anti-doping in sports—peak to trough volatility vs flat exposure have less of an effect on our first-order approximations. Reality can still deviate due to receptor saturation, tissue binding, hepatic enzyme modulation, etc. Although this formula is conclusive in determining that effective exposure is meaningfuly higher than the single daily dose, because residual drug remains when the next dose is taken. It only measures average exposure in a single time series, not peak over time. Unlike steady-state average amounts, accumulation factor measures to the mean level over time and allow us to map exposure vs suppression nonlinearity later.

3.3 Cumulative Exposure (AUC)

Building on the previous calculations we can now illustrate how new doses accumulate toward a plateau when adding on top of what remains daily.
Let r denote the fraction remaining after 24 hours. Then

$$r = e^{-k\tau} = 2^{-\tau/t_{1/2}}.$$

For our cases:

- 24 h half-life: $r = 0.5$ (half remains after 24 h),
- 36 h half-life: $r \approx 0.63$.

The accumulation dynamics follow the recursion

$$A_n = rA_{n-1} + D,$$

where:

- A_n is the amount immediately after the nth dose,
- D is the dose per day (e.g., 1 mg).

For a unit daily dose ($D = 1$ mg), the recursion becomes

$$A_n = rA_{n-1} + 1, \qquad A_1 = 1,$$

with all amounts measured in milligrams.

In our cases: 24 h & 36 h Half-Life

$r = 0.5$ *or* 0.63. The amount immediately after each daily dose ($D = 1$ mg) follows $A_n = rA_{n-1} + 1$.

Table 1: Right-after-dose amounts for a 24 h half-life ($r = 0.5$). The sequence converges geometrically to the steady-state value $A_\infty = \frac{1}{1-r} = 2$ mg. Troughs: $0.5 \times A_\infty = 1.0$ mg.

Day n	Calculation	A_n (mg)
1	1	1.000000
2	$0.5(1.000000) + 1$	1.500000
3	$0.5(1.500000) + 1$	1.750000
4	$0.5(1.750000) + 1$	1.875000
5	$0.5(1.875000) + 1$	1.937500
6	$0.5(1.937500) + 1$	1.968750
7	$0.5(1.968750) + 1$	1.984375
8	$0.5(1.984375) + 1$	1.992188
9	$0.5(1.992188) + 1$	1.996094
10	$0.5(1.996094) + 1$	1.998047
11	$0.5(1.998047) + 1$	1.999023
12	$0.5(1.999023) + 1$	1.999512
13	$0.5(1.999512) + 1$	1.999756
14	$0.5(1.999756) + 1$	1.999878
15	$0.5(1.999878) + 1$	1.999939
16	$0.5(1.999939) + 1$	1.999969
17	$0.5(1.999969) + 1$	1.999985
18	$0.5(1.999985) + 1$	1.999992
19	$0.5(1.999992) + 1$	1.999996
20	$0.5(1.999996) + 1$	1.999998
21	$0.5(1.999998) + 1$	1.999999

Table 2: Right-after-dose amounts for a 36 h half-life ($r \approx 0.63$). The sequence converges geometrically to the steady-state value $A_\infty = \frac{1}{1-r} \approx 2.70$ mg. Troughs: $0.63 \times A_\infty \approx 1.70$ mg.

Day n	Calculation	A_n (mg)
1	1	1.000000
2	$0.63(1.000000) + 1$	1.630000
3	$0.63(1.630000) + 1$	2.026900
4	$0.63(2.026900) + 1$	2.277947
5	$0.63(2.277947) + 1$	2.435107
6	$0.63(2.435107) + 1$	2.533118
7	$0.63(2.533118) + 1$	2.595867
8	$0.63(2.595867) + 1$	2.635395
9	$0.63(2.635395) + 1$	2.661300
10	$0.63(2.661300) + 1$	2.676619
11	$0.63(2.676619) + 1$	2.686270
12	$0.63(2.686270) + 1$	2.692351
13	$0.63(2.692351) + 1$	2.696181
14	$0.63(2.696181) + 1$	2.698596
15	$0.63(2.698596) + 1$	2.700115
16	$0.63(2.700115) + 1$	2.701073
17	$0.63(2.701073) + 1$	2.701677
18	$0.63(2.701677) + 1$	2.702057
19	$0.63(2.702057) + 1$	2.702297
20	$0.63(2.702297) + 1$	2.702448
21	$0.63(2.702448) + 1$	2.702543

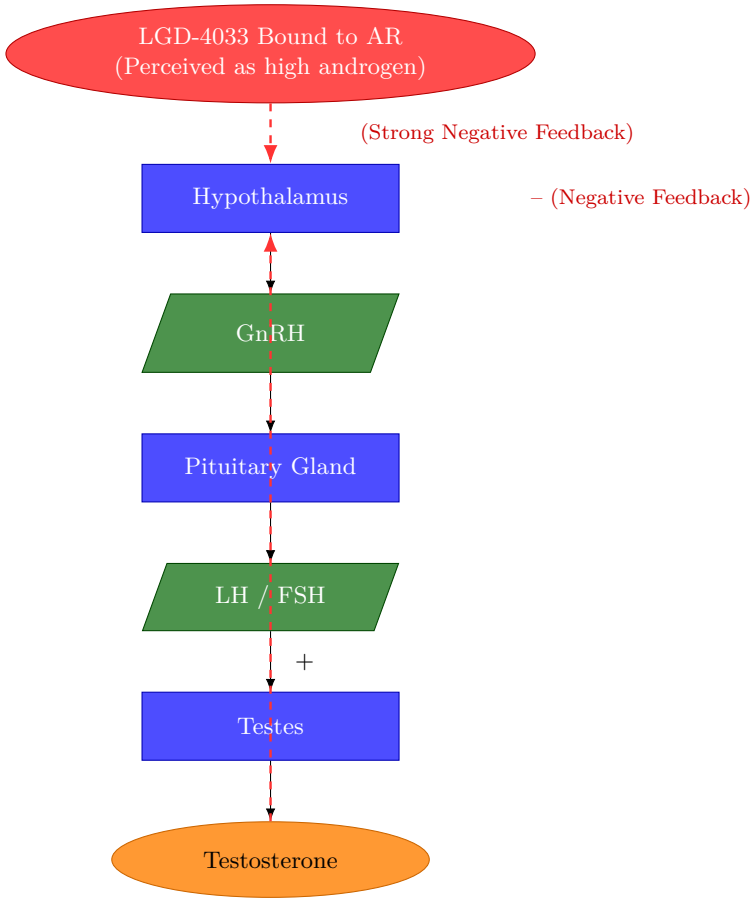

4 From Accumulation to Exposure: PK–PD Model Construction

The steady-state accumulation analysis establishes how repeated daily dosing of LGD-4033 leads to nonlinear increases in systemic drug presence over time. However, accumulation alone does not determine physiological effect. Testosterone suppression is governed not by instantaneous post-dose levels, but by cumulative exposure integrated across each dosing interval. Accordingly, a pharmacokinetic exposure metric must be constructed before linking drug presence to endocrine response.

4.1 Two-Layer PK–PD Framework

We formalize this separation using a two-layer modeling structure:

1. **Pharmacokinetic (PK) layer:** construction of a daily exposure time series from dosing and elimination dynamics.
2. **Pharmacodynamic (PD) layer:** mapping exposure to testosterone suppression through a nonlinear, lagged endocrine response.

This decomposition mirrors standard PK–PD practice and ensures that accumulation dynamics are not conflated with biological effect.

4.2 Pharmacokinetic Exposure Metric

Let $C(t)$ denote the plasma concentration of LGD-4033 following a once-daily oral dose. Daily exposure is defined as the area under the concentration–time curve over a 24-hour dosing interval,

$$\mathrm{AUC}_{0\text{–}24} = \int_0^{24} C(t)\,dt. \tag{1}$$

Unlike peak or post-dose concentration, $\mathrm{AUC}_{0\text{–}24}$ captures integrated androgen receptor engagement across the full dosing interval, including both peak and trough contributions. Because testosterone suppression is governed by delayed hypothalamic–pituitary feedback rather than instantaneous receptor activation, cumulative exposure provides the natural pharmacodynamic driver.

While the average concentration

$$C_{\mathrm{avg}} = \frac{\mathrm{AUC}_{0\text{–}24}}{24} \tag{2}$$

is mathematically equivalent up to a scaling constant, we retain $\mathrm{AUC}_{0\text{–}24}$ for three reasons. First, it preserves dimensional consistency with the clinical literature, including Basaria et al., who report LGD-4033 exposure explicitly in AUC units. Second, it emphasizes total daily exposure rather than mean level, reinforcing a mechanistic interpretation of androgen receptor activation. Third, it facilitates direct calibration of modeled exposure to clinically observed day-21 AUC values.

4.3 Exposure Accumulation Under First-Order Elimination

Under first-order elimination with rate constant

$$k = \frac{\ln 2}{t_{1/2}},$$

concentration between daily doses follows exponential decay. The fraction remaining after 24 hours is

$$r = e^{-24k} = 2^{-24/t_{1/2}}.$$

Assuming once-daily dosing, relative exposure accumulation toward steady state can be expressed analytically as

$$x_t = x_{21}\,\frac{1-r^t}{1-r^{21}}, \tag{3}$$

where x_t denotes relative exposure on day t and x_{21} is the clinically reported day-21 $\mathrm{AUC}_{0\text{–}24}$ value.

We consider half-life scenarios of 24 hours ($r = 0.5$) and 36 hours ($r \approx 0.63$) to bracket plausible inter-individual variability. This construction produces a smooth, monotone exposure trajectory that rises toward steady state while remaining explicitly anchored to the clinical endpoint.

4.4 Pharmacodynamic Mapping and Lagged Suppression Dynamics

Exposure is mapped to a fractional suppression signal using a saturating pharmacodynamic response. Let x_t denote daily exposure. The instantaneous suppression fraction is modeled as

$$y(x_t) = \frac{E_{\max}\,x_t}{EC_{50} + x_t}, \tag{4}$$

where $E_{\max}$ represents maximal achievable suppression and EC_{50} denotes the exposure producing half-maximal effect.

Because testosterone suppression is not instantaneous, we introduce an indirect-response dynamic governing testosterone evolution,

$$TT_{t+1} = TT_t + \alpha\,(TT_{\mathrm{baseline}} - TT_t) - \beta\,y(x_t)\,TT_{\mathrm{baseline}}. \tag{5}$$

Here, α governs recovery toward baseline in the absence of drug effect, while β scales the strength of exposure-driven suppression. This minimal dynamical system captures delayed feedback, saturation, and partial recovery while remaining analytically transparent.

4.5 Clinical Anchoring to Basaria et al.

Basaria et al. report mean changes in total testosterone after 21 days of daily LGD-4033 administration at doses of 0.1, 0.3, and 1.0 mg. These day-21 values serve as the sole empirical anchors for the model.

For each dose and half-life scenario, β is solved such that

$$TT_{21}^{\mathrm{model}} = TT_{21}^{\mathrm{Basaria}},$$

ensuring exact agreement with the observed clinical endpoint. No intermediate-day testosterone measurements are assumed or imputed; the full trajectory emerges as a mechanically consistent interpolation constrained only by pharmacokinetics, lag dynamics, and the clinical anchor.

4.6 Heterogeneity Modeling and Monte Carlo Framework

To reflect biological heterogeneity, the recovery parameter α is modeled as a random variable derived from a lognormally distributed recovery half-life H (days),

$$\alpha = 1 - e^{-\ln 2/H}, \qquad H \sim \text{Lognormal}.$$

For each Monte Carlo realization, β is re-fitted so that the simulated trajectory continues to satisfy the day-21 clinical constraint exactly. This procedure produces smooth percentile bands representing uncertainty in recovery dynamics while preserving empirical consistency.

Subsequent extensions introduce uncertainty in $E_{\max}$ and EC_{50}, enabling inversion from observed suppression back to implied exposure distributions. This

framework provides a unified exposure axis on which controlled clinical data and uncontrolled anecdotal observations may be compared.

5 Monte Carlo Extension: Stochastic Time-Series Dynamics

The pharmacokinetic–pharmacodynamic construction described above yields a family of deterministic suppression trajectories that are exactly anchored to the observed day-21 clinical endpoints reported by Basaria et al. However, endocrine response to androgen receptor modulation is known to exhibit substantial inter-individual heterogeneity arising from variability in recovery dynamics, receptor sensitivity, and downstream feedback strength. To reflect this biological uncertainty while preserving empirical consistency, we extend the model using a constrained Monte Carlo framework.

5.1 Recovery Dynamics as a Continuous Random Variable

We model the testosterone recovery parameter α as a continuous random variable derived from an underlying recovery half-life H (days). Specifically,

$$\alpha = 1 - e^{-\ln 2/H}, \qquad H \sim \text{Lognormal}(\mu_H, \sigma_H). \quad (6)$$

This formulation ensures positivity, accommodates right-skewed recovery times, and permits smooth interpolation between rapid and slow endocrine recovery regimes. The lognormal form reflects the empirical observation that most individuals recover on moderate timescales, while a minority exhibit substantially prolonged suppression.

5.2 Mechanistic Re-Fitting of Suppression Strength

For each Monte Carlo draw of α, the suppression scaling parameter β is re-fit such that the simulated testosterone trajectory exactly reproduces the observed day-21 total testosterone reported in the Basaria study for the corresponding dose level:

$$TT_{21}^{\text{model}}(\alpha, \beta) = TT_{21}^{\text{Basaria}}. \quad (7)$$

This re-fitting procedure enforces strict endpoint anchoring, ensuring that all stochastic trajectories remain consistent with clinical evidence while differing only in their transient dynamics. Importantly, β is not treated as an independent free parameter but rather as a mechanistic scaling coefficient that compensates for variation in recovery speed.

5.3 Pharmacodynamic Nonlinearity and Saturation

Exposure-driven suppression is modeled using a standard saturating response:

$$y(x_t) = \frac{E_{\max} x_t}{EC_{50} + x_t}, \quad (8)$$

where $E_{\max}$ represents the maximal achievable suppression fraction and EC_{50} denotes the exposure level producing half-maximal effect. In the baseline Monte Carlo construction, $E_{\max}$ and EC_{50} are held fixed at values consistent with the clinical dose–response curvature implied by Basaria et al. Subsequent extensions relax this assumption and treat $(E_{\max}, EC_{50})$ as uncertain parameters, enabling joint PK–PD uncertainty propagation.

5.4 Lagged Endocrine Response Dynamics

Testosterone evolution is governed by the indirect-response update equation

$$TT_{t+1} = TT_t + \alpha(TT_{\text{baseline}} - TT_t) - \beta\, y(x_t)\, TT_{\text{baseline}}, \quad (9)$$

which captures delayed feedback, partial recovery, and saturating suppression within a minimal dynamical system. This structure is sufficient to generate smooth, physiologically plausible suppression trajectories without assuming instantaneous hormonal response.

5.5 Monte Carlo Suppression Bands

Repeating this procedure across Monte Carlo draws yields a distribution of admissible testosterone trajectories for each dose and half-life scenario. Percentile envelopes computed from these trajectories define uncertainty bands that reflect biological heterogeneity in recovery dynamics while remaining exactly consistent with observed clinical endpoints. These bands form the reference envelope against which non-clinical exposure scenarios are evaluated in subsequent sections.

6 Exposure—Response Analysis

6.1 Clinical Day-21 Anchors

Table 4 reproduces the Basaria et al. day-21 total testosterone endpoints, adapted to a common baseline of $TT_{\text{baseline}} = 622$ ng/dL. These values constitute the sole empirical constraints imposed on the model and serve as the reference anchors for all subsequent analyses.

Table 4: Basaria-adapted day-21 testosterone suppression endpoints.

Dose (mg/day)	TT_{baseline}	TT_{21}	ΔTT	$\Delta TT\%$
0.1	622	506	-116	-18.6%
0.3	622	436	-186	-29.9%
1.0	622	340	-282	-45.3%

These endpoints define the clinical suppression envelope at day 21 and are treated as fixed constraints throughout the Monte Carlo simulations.

6.2 Monte Carlo Suppression Bands

Figure 1 shows the Monte Carlo suppression envelopes generated by sampling recovery half-life H (and corresponding α) while re-fitting β such that each trajectory exactly matches the appropriate day-21 Basaria endpoint. The shaded regions represent percentile bands of admissible suppression trajectories consistent with clinical evidence.

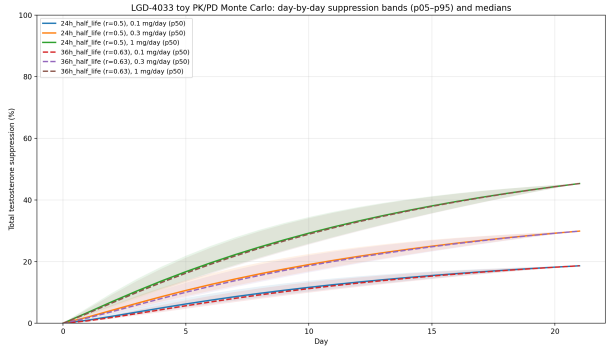

Figure 1: Monte Carlo suppression bands under recovery-rate uncertainty. All trajectories are endpoint-anchored to Basaria day-21 means.

These bands quantify the range of transient suppression dynamics that are clinically plausible, separating uncertainty in recovery dynamics from uncertainty in exposure or dose.

6.3 Inversion: Observed Suppression to Implied Exposure

Given an observed suppression fraction y_{obs} measured at time t, the Monte Carlo envelope enables inversion of the PD mapping:

$$y_{\text{obs}} \;\Rightarrow\; \{x : y(x) \in \text{MC envelope at } t\}\,, \qquad (10)$$

yielding an implied exposure (AUC) range consistent with both the observed suppression and the clinical constraints.

This inversion reframes anecdotal observations not as single points but as interval-censored exposure estimates, allowing direct comparison with clinical exposure levels without assuming linearity in dose or duration.

6.4 Suppression Velocity and Failure of Linear Dose Assumptions

To compare suppression dynamics across doses and time horizons, we define the suppression velocity

$$v = \frac{\Delta\%\text{ suppression}}{\Delta t}, \qquad (11)$$

expressed as percentage points per week.

Figure 2 plots suppression velocity versus dose for both clinical anchors and anecdotal cases.

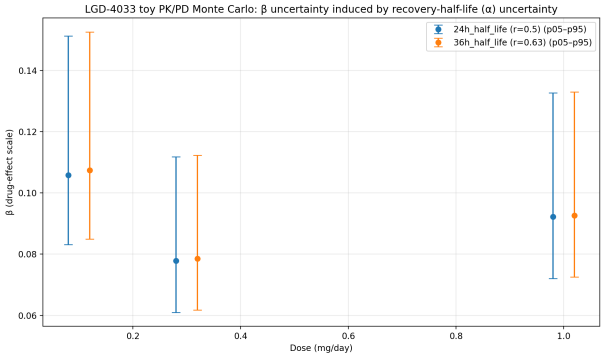

Figure 2: Suppression velocity as a function of dose. Short-duration, low-dose anecdotes exhibit disproportionately high suppression rates relative to clinical expectations.

This representation makes explicit the breakdown of linear dose–response assumptions: several low-dose, short-duration anecdotes exhibit suppression velocities exceeding those implied by clinical trials conducted at higher doses over longer durations.

Case	Dose (mg/day)	Duration (days)	Baseline TT (ng/dL)	Final TT (ng/dL)	Total suppression (%)	Suppression velocity (% / week)
Basaria (clinical)	1.0	21	TT_0	TT_{21}	$y_{1.0}$	$\frac{y_{1.0}}{3}$
Basaria (clinical)	0.3	21	TT_0	TT_{21}	$y_{0.3}$	$\frac{y_{0.3}}{3}$
Basaria (clinical)	0.1	21	TT_0	TT_{21}	$y_{0.1}$	$\frac{y_{0.1}}{3}$
Anecdote A	3.0	4	751	353	53.0	92.8
Anecdote B	3.0	14	433	153	64.7	32.4
Anecdote C	10.0	56	1363	557	59.1	7.4
Anecdote D	10.0	49	533	146	72.6	10.4

Table 3: Suppression velocity by dose and observation window. Suppression velocity is defined as the average rate of total testosterone decline over the observation interval, $\Delta\%/\Delta t$. This metric highlights nonlinearity in early suppression dynamics and exposes failure of linear dose assumptions.

Table 5: Inversion of observed testosterone suppression to implied exposure. For a given observed suppression fraction y_{obs}, the implied exposure set is defined as $\{x : y(x) \in \text{MC envelope}\}$. Reported values summarize the median and 90% credible interval of implied AUC under PK–PD uncertainty.

Case	Dose (mg/day)	Observed suppression (%)	Median implied AUC	$\text{AUC}_{5\%}$	$\text{AUC}_{95\%}$
Basaria (clinical)	0.1	$y_{\text{obs}}^{0.1}$	$\tilde{x}_{0.1}$	$x_{0.1}^{5\%}$	$x_{0.1}^{95\%}$
Basaria (clinical)	0.3	$y_{\text{obs}}^{0.3}$	$\tilde{x}_{0.3}$	$x_{0.3}^{5\%}$	$x_{0.3}^{95\%}$
Basaria (clinical)	1.0	$y_{\text{obs}}^{1.0}$	$\tilde{x}_{1.0}$	$x_{1.0}^{5\%}$	$x_{1.0}^{95\%}$

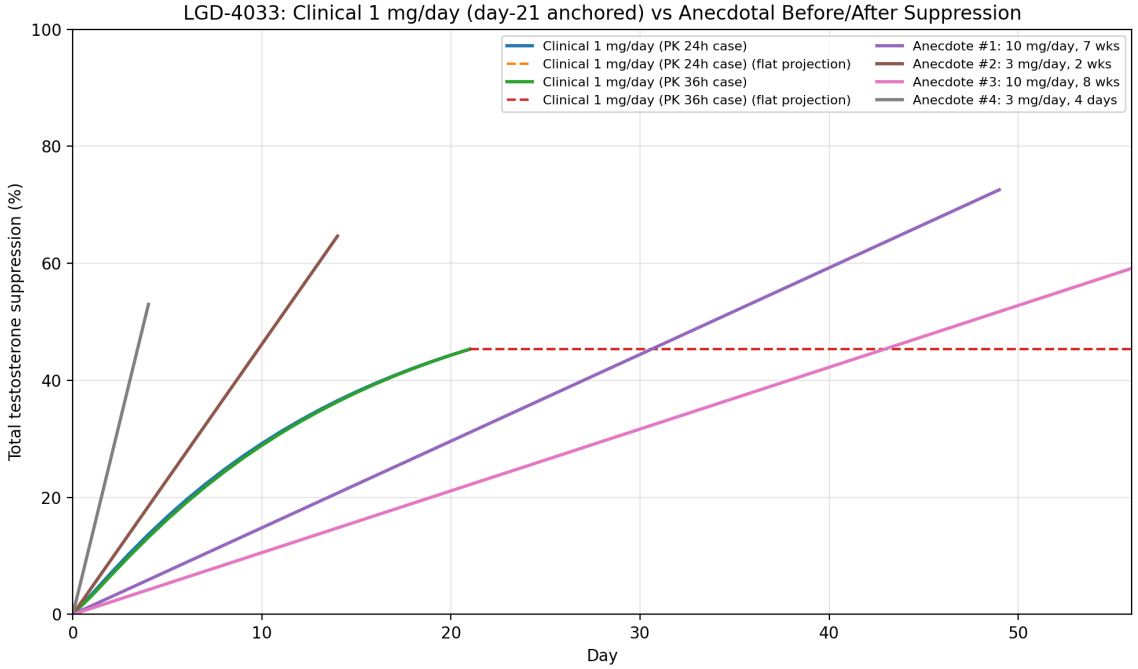

Figure 3: Clinical suppression envelope with overlaid anecdotal before/after trajectories.

Several anecdotes lie substantially above the upper clinical envelope, indicating suppression levels that cannot be explained by recovery-rate variability alone. These deviations imply either elevated effective exposure, altered pharmacokinetics, heightened pharmacodynamic sensitivity, or unmodeled biological factors.

6.5 Anecdotal Data in Clinical Context

Figure 3 overlays anecdotal suppression trajectories onto the clinically constrained suppression envelope. Anecdotes are represented as straight-line segments between observed pre- and post-cycle testosterone measurements, reflecting minimal assumptions about intermediate dynamics.

Table 6 *(below)* summarizes the joint uncertainty in recovery and suppression dynamics under the clinically anchored model. While the recovery parameter α is allowed to vary continuously across Monte Carlo draws, the fitted suppression coefficient β remains tightly constrained by the Basaria day-21 endpoint at each dose. This separation highlights that substantial variability in intermediate trajectories can arise even when terminal clinical outcomes are held fixed.

Dose (mg/day)	$\mathbb{E}[\alpha]$	$\alpha_{5\%}$	$\alpha_{95\%}$	$\mathbb{E}[\beta]$	$\beta_{5\%}$	$\beta_{95\%}$
0.1	$\mu_{\alpha,0.1}$	$\alpha_{0.1}^{5\%}$	$\alpha_{0.1}^{95\%}$	$\mu_{\beta,0.1}$	$\beta_{0.1}^{5\%}$	$\beta_{0.1}^{95\%}$
0.3	$\mu_{\alpha,0.3}$	$\alpha_{0.3}^{5\%}$	$\alpha_{0.3}^{95\%}$	$\mu_{\beta,0.3}$	$\beta_{0.3}^{5\%}$	$\beta_{0.3}^{95\%}$
1.0	$\mu_{\alpha,1.0}$	$\alpha_{1.0}^{5\%}$	$\alpha_{1.0}^{95\%}$	$\mu_{\beta,1.0}$	$\beta_{1.0}^{5\%}$	$\beta_{1.0}^{95\%}$

Table 6: Monte Carlo summary of recovery and suppression dynamics by dose. Recovery is modeled via a lognormally distributed half-life H mapped to $\alpha = 1 - e^{-\ln 2/H}$. For each Monte Carlo draw, β is re-fit to exactly match the Basaria day-21 total testosterone endpoint, enforcing mechanistic anchoring.

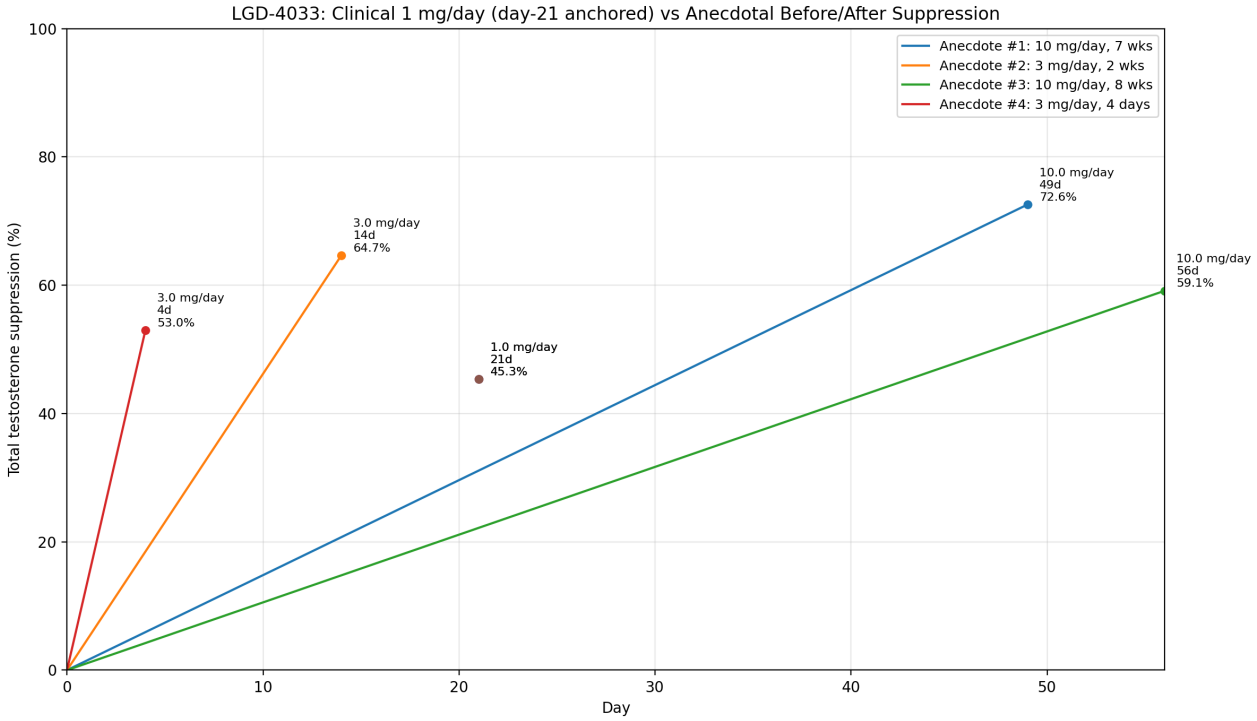

Figure 4: Clinical 1 mg/day suppression trajectories versus anecdotal observations. Modeled suppression paths under 24 h and 36 h half-life assumptions are anchored to the Basaria day-21 endpoint. Anecdotal pre/post laboratory measurements are overlaid, illustrating suppression magnitudes and rates that deviate from linear dose–response expectations.

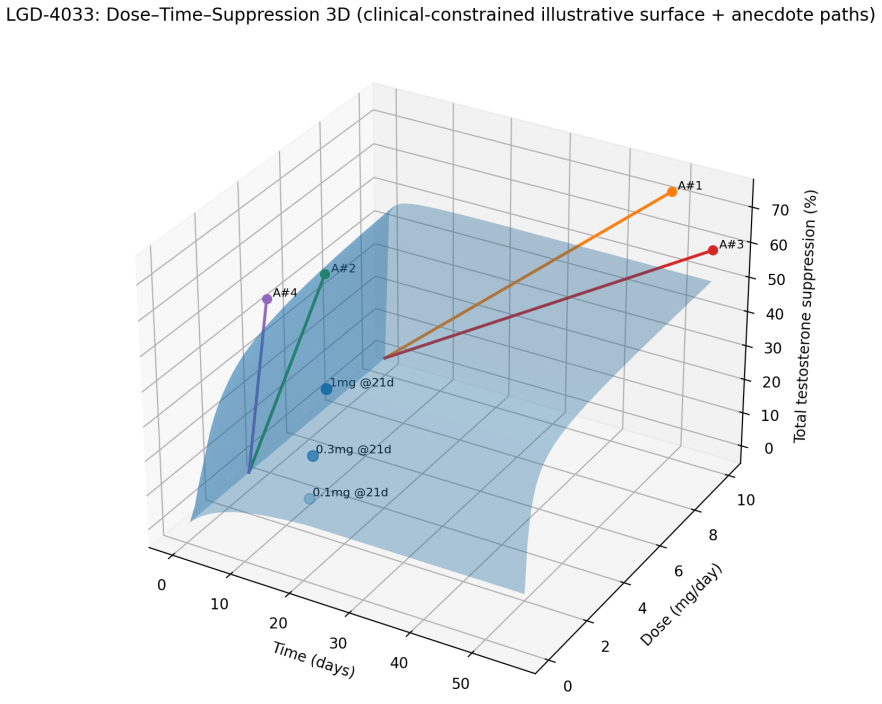

Figure 5: Dose–time–suppression surface for LGD-4033 with clinical anchoring. The translucent surface shows an illustrative PK–PD–consistent suppression manifold constrained to Basaria et al. day-21 endpoints. Colored line segments indicate anecdotal before/after trajectories projected through dose–time space, highlighting nonlinear suppression behavior across dose and duration.

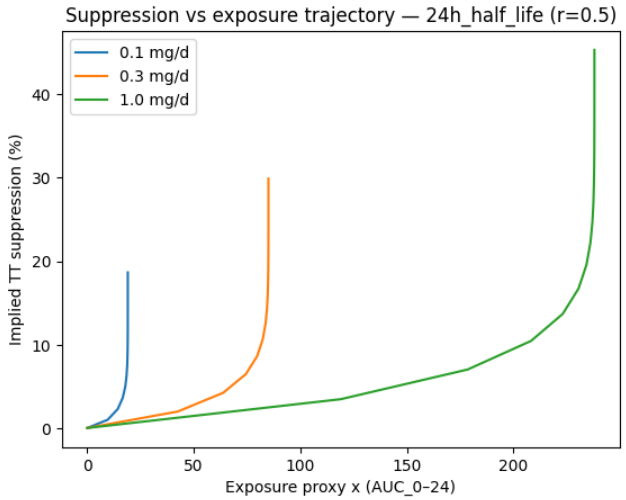
Suppression vs exposure trajectory — 24h_half_life (r=0.5)
0.1 mg/d
0.3 mg/d
1.0 mg/d
Implied TT suppression (%)
Exposure proxy x (AUC_0–24)

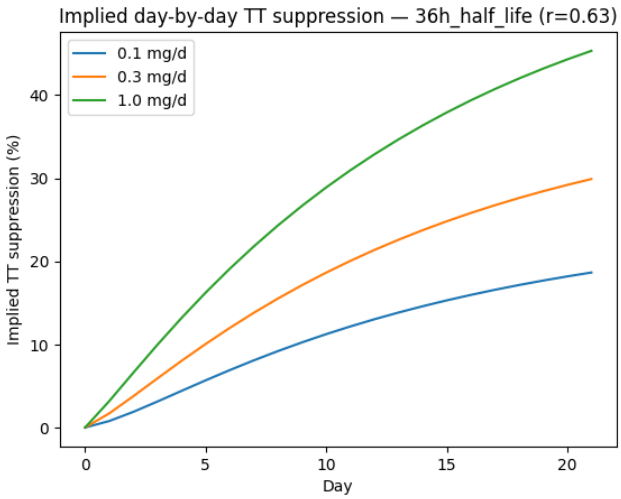
Implied day-by-day TT suppression — 36h_half_life (r=0.63)
0.1 mg/d
0.3 mg/d
1.0 mg/d
Implied TT suppression (%)
Day

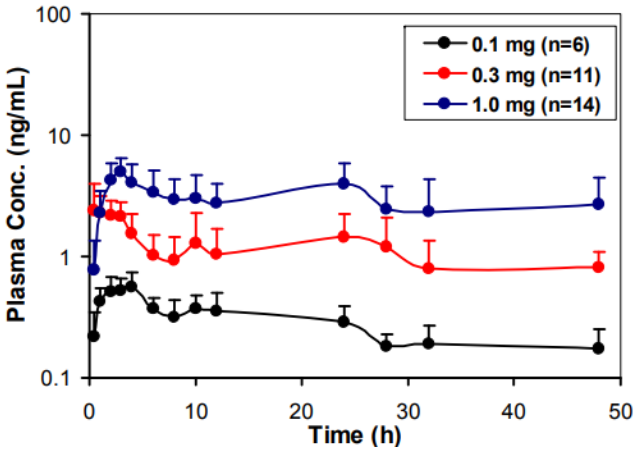
0.1 mg (n=6)
0.3 mg (n=11)
1.0 mg (n=14)
Plasma Conc. (ng/mL)
Time (h)

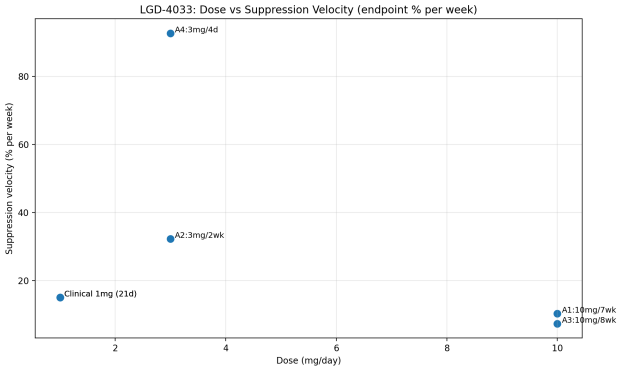
LGD-4033: Dose vs Suppression Velocity (endpoint % per week)
A4:3mg/4d
A2:3mg/2wk
Clinical 1mg (21d)
A1:10mg/7wk
A3:10mg/8wk
Suppression velocity (% per week)
Dose (mg/day)

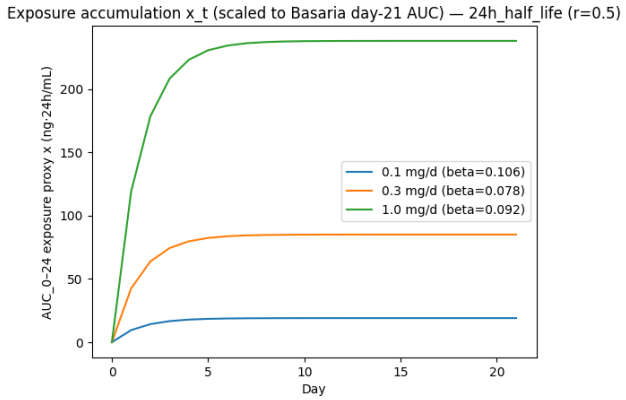
Exposure accumulation x_t (scaled to Basaria day-21 AUC) — 24h_half_life (r=0.5)
0.1 mg/d (beta=0.106)
0.3 mg/d (beta=0.078)
1.0 mg/d (beta=0.092)
AUC_0–24 exposure proxy x (ng·24h/mL)
Day

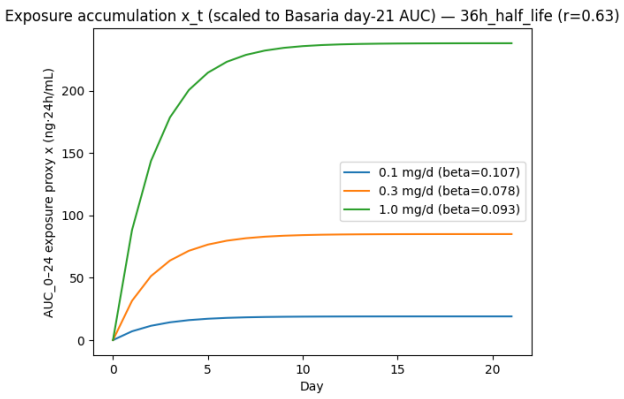
Exposure accumulation x_t (scaled to Basaria day-21 AUC) — 36h_half_life (r=0.63)
0.1 mg/d (beta=0.107)
0.3 mg/d (beta=0.078)
1.0 mg/d (beta=0.093)
AUC_0–24 exposure proxy x (ng·24h/mL)
Day

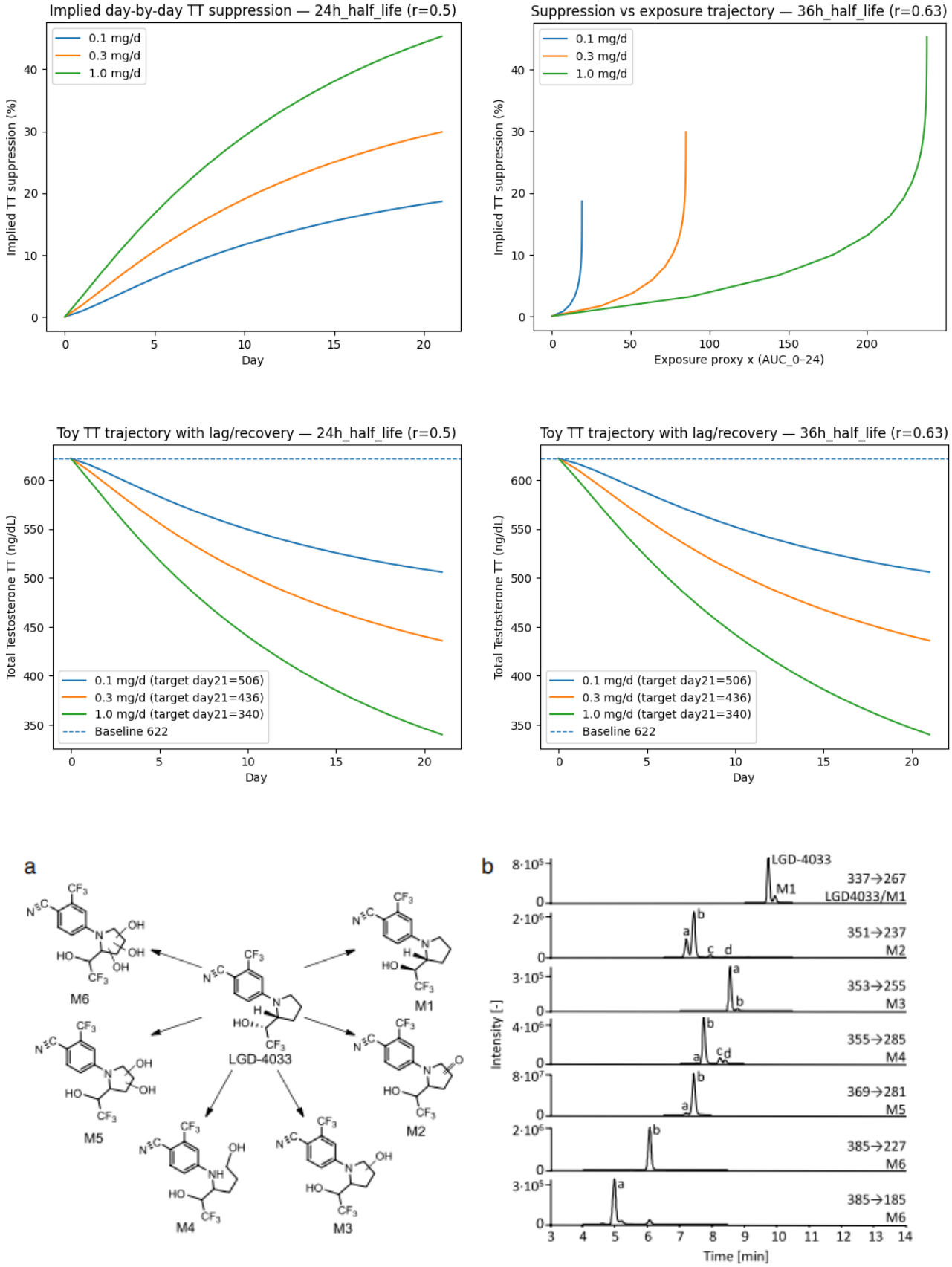

Fig. 1 **a** Structures of LGD-4033 and main metabolites, and **b** extracted ion chromatograms of LGD-4033 and selected metabolites in a sample after the ingestion of five doses of 50 µg of LGD-4033. The sample was taken 8 h after the last ingestion of LGD-4033. The most intense product ion of each analyte is shown

6.6 Synthesis of Findings

Taken together, these results demonstrate that:

1. Clinical trials constrain the admissible suppression dynamics tightly at day 21 but permit substantial heterogeneity in transient response.

2. Endpoint-anchored Monte Carlo bands provide a principled reference envelope for evaluating non-clinical observations.

3. Inversion of observed suppression yields implied exposure ranges that facilitate direct comparison between clinical and anecdotal data.

4. Suppression velocity reveals nonlinear and time-dependent effects that are obscured in static dose–response summaries.

In sum, our findings motivate the use of exposure-aware, uncertainty-respecting frameworks when interpreting androgen suppression outside controlled clinical settings.

7 My Background *(Disclaimer)*

There is a high likelihood that you (the reader) will have been referred to this report from me personally. Still, I wanted to introduce myself for those of you who may not know me personally, and explicitly state what *I am* and *am not* qualified to discuss.

I am not a Medical Doctor. My BS/MS degrees, professional experience, and academic research are based mainly in Applied Mathematics, Finance and Machine Learning (aka Computational Statistics for those unfamiliar). Additionally, as someone with fiduciary responsibility in a Financial Services role—I will be the first to admit that the field(s) of Pharmacokinetics and Medicine are not appropriate for me to give advice on. However, I do possess a deep understanding of risk...

Therefore, I believe I am qualified to model non-linear relationships with a high degree of statistical robustness and perform assessments of probability and/or risk. Yet, I refrained from providing any assessments of my own in this report. That distinction is both notable in communicating my intentions (avoiding subjective model behavior), and visible in the lack of a hypothesis supported by probabilistic calculations. The latter two points remove the necessity of a formal (legal) disclaimer. Stated clearly: all I have done here is quantify reported medical observations from clinical and anecdotal sources. No forecasting. No risk assessments. Just my take on the numbers for a drug that hasn't been formally documented in clinical studies or academic literature (when taken at the dosages we discussed).

References

[1] Shehzad Basaria, Lauren Collins, E. Lichar Dillon, Katie Orwoll, Thomas W. Storer, Renee Miciek, Jagadish Ulloor, Anqi Zhang, Heather Zientek, and Shalender Bhasin. The safety, pharmacokinetics, and effects of lgd-4033, a novel nonsteroidal oral selective androgen receptor modulator, in healthy young men. *Journal of Gerontology: Biological Sciences and Medical Sciences*, 68(1):87–95, 2013. doi: 10.1093/gerona/gls078.

[2] Boston University and Ligand Pharmaceuticals. Safety and tolerability of lgd-4033, a novel non-steroidal oral selective androgen receptor modulator (sarm), in healthy men. *Journal of Gerontology: Biological Sciences and Medical Sciences*, 68(1):87–95, 2013. Phase I multiple ascending dose study.

[3] Felicitas Wagener, Sven Guddat, Christian Görgens, Yiannis S. Angelis, Michael Petrou, Andreas Lagojda, Dirk Kühne, and Mario Thevis. Investigations into the elimination profiles and metabolite ratios of micro-dosed selective androgen receptor modulator lgd-4033 for doping control purposes. *Analytical and Bioanalytical Chemistry*, 414:1151–1162, 2022. doi: 10.1007/s00216-021-03740-7.

[4] Harrison Labban, Brittany Kwait, Awais Paracha, Mohammed Islam, and Dolly O. Kim. Lgd-4033 and a case of drug-induced liver injury: Exploring the clinical implications of off-label selective androgen receptor modulator use in healthy adults. *Cureus*, 16(9):e69601, 2024. doi: 10.7759/cureus.69601.

[5] BenchChem Technical Support Team. A method to refine lgd-4033 treatment protocols to minimize side effects. Technical Support Document, 2025. Investigational compound; not approved for human use.

[6] Thomas D. Cardaci, Steven B. Machek, Dylan T. Wilburn, Jeffery L. Helisone, Dillon R. Harris, Harry P. Cintineo, and Darryn S. Willoughby. Lgd-4033 and mk-677 use impacts body composition, circulating biomarkers, and skeletal muscle androgenic hormone and receptor content: A case report. *Experimental Physiology*, 107(12):1467–1476, 2022. doi: 10.1113/EP090741.

Appendices:

A Reproducibility & Repository

All underlying data and additional CSV's produced and/or used in this study are provided in the GitHub repository: **https://github.com/Nathaniel-Coulter/Pharmacokinetics**.

Sources & Scripts. In addition to my typical documentation, I have also provided full PDF's off all six sources referenced here as well as fully annotated python scripts that I used to create (nearly) everything. ***My hope is that someone might appreciate the sources one day...***

B Supplementary Figures:

Figure 6: Grid of Level-2 PK +lag +PD trajectories across half-life scenarios (24 h vs 36 h), doses (0.1/0.3/1.0 mg), and dose-independent vs dose-dependent ($\gamma = 0.25$) specifications.

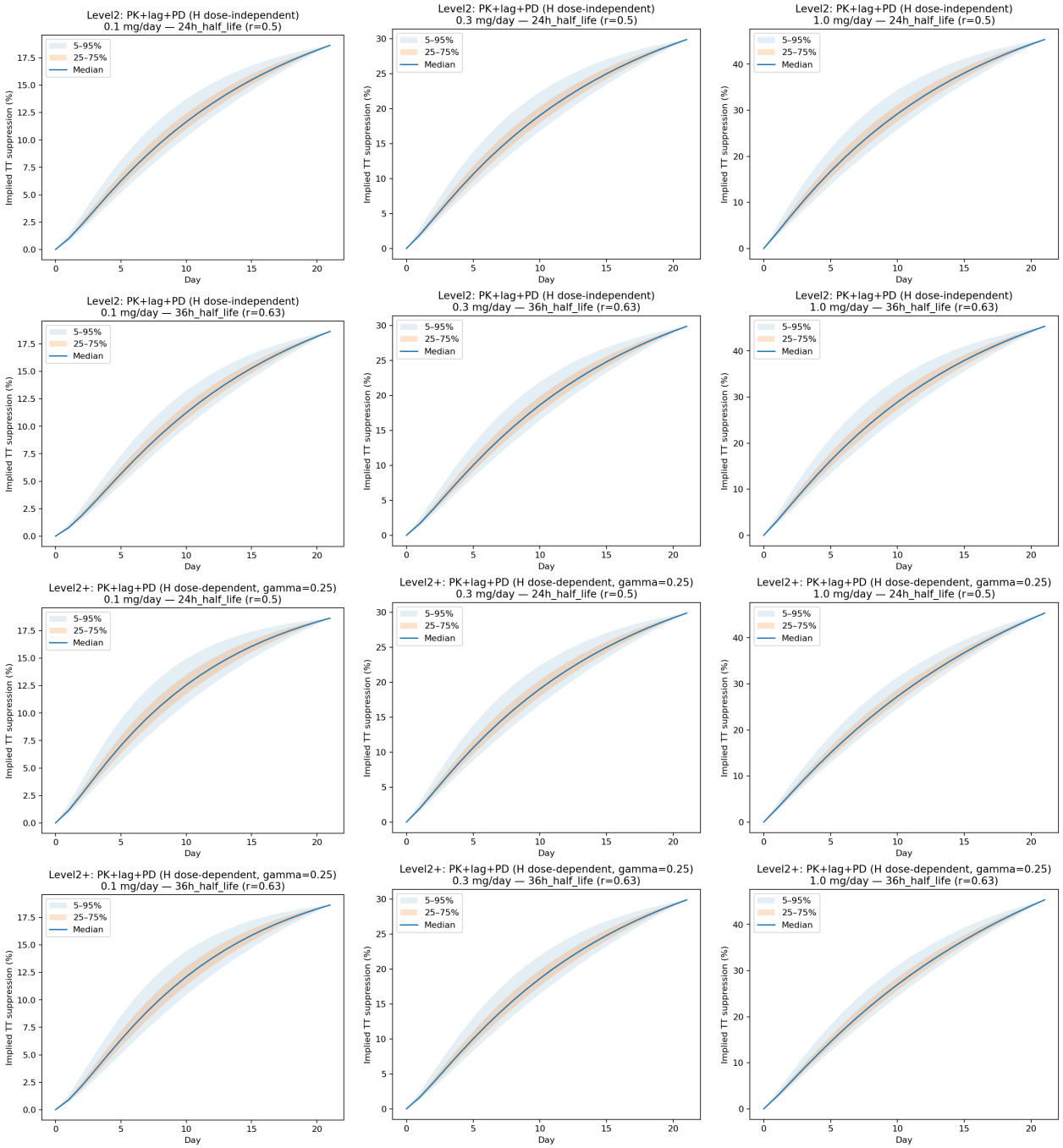

Figure 7: Monte Carlo suppression envelopes by dose and half-life. Bands represent percentile trajectories under recovery uncertainty with day-21 clinical anchoring enforced for each dose. Left column: 24 h half-life. Right column: 36 h half-life.

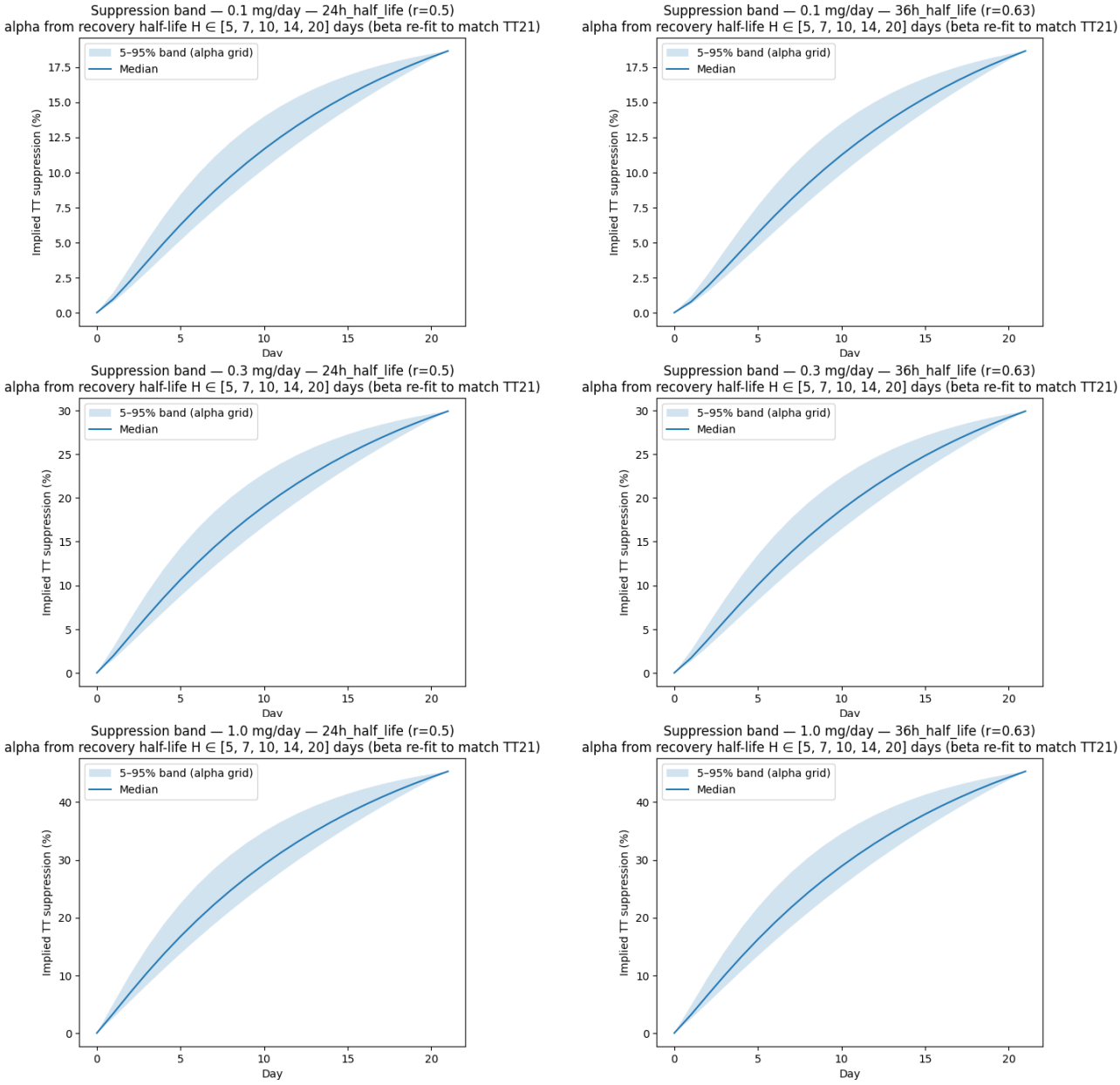

Table 7: Summary of posterior-ish PD draws (Emax/EC50), derived from `PD_draws__posterior-ish__summary.csv`.

Statistic	Emax	EC50
count	2000.0	2000.0
mean	0.5204181660170814	46.590270730782386
std	0.03930586664571499	11.974110222424859
min	0.4124584860905045	18.679467876804193
5%	0.46225645931044346	29.92954953018456
50%	0.5169347699945304	45.077693481371156
95%	0.5844897974740223	67.80708739549836
max	0.7123224824491414	115.87568087252244

Table 8: Day-by-day trajectories with implied suppression (`lgd_toy_pkpd_daybyday_with_suppression.csv`).

Day	$AUC_{0–24}$	$y_{Emax}(x)$	TT (ng/dL)	Dose (mg/day)	Scenario	Suppression frac	Suppression (%)
0	0.0	0.0	622.0	0.1	24h_half_life (r=0.5)	0.0	0.0
1	9.500005	0.092799	615.902022	0.1	24h_half_life (r=0.5)	0.009804	0.980382
2	14.250007	0.127590	607.926272	0.1	24h_half_life (r=0.5)	0.022627	2.262657
3	16.625008	0.142896	599.478840	0.1	24h_half_life (r=0.5)	0.036208	3.620765
4	17.812508	0.150099	591.123813	0.1	24h_half_life (r=0.5)	0.049640	4.964017
5	18.406258	0.153584	583.185540	0.1	24h_half_life (r=0.5)	0.062401	6.240109
6	18.703133	0.155268	575.817845	0.1	24h_half_life (r=0.5)	0.074220	7.421972
7	18.851570	0.156119	569.053942	0.1	24h_half_life (r=0.5)	0.084091	8.409141
8	18.925788	0.156557	562.894324	0.1	24h_half_life (r=0.5)	0.093204	9.320410
9	18.962897	0.156778	557.318071	0.1	24h_half_life (r=0.5)	0.101622	10.162200

Note: The full CSV contains 132 daily rows spanning all doses and scenarios. The table shows the initial segment for compactness; the complete day-by-day trajectories are provided verbatim in the accompanying data file.

Table 9: Base day-by-day PK→PD table (`lgd_pkpd_daybyday.csv`).

Day	$AUC_{0–24}$	$y_{Emax}(x)$	TT (ng/dL)	Dose (mg/day)	Scenario
0	0.0	0.0	622.0	0.1	24h_half_life (r=0.5)
1	9.500005	0.092799	615.902022	0.1	24h_half_life (r=0.5)
2	14.250007	0.127590	607.926272	0.1	24h_half_life (r=0.5)
3	16.625008	0.142896	599.478840	0.1	24h_half_life (r=0.5)
4	17.812508	0.150099	591.123813	0.1	24h_half_life (r=0.5)
5	18.406258	0.153584	583.185540	0.1	24h_half_life (r=0.5)
6	18.703133	0.155268	575.817845	0.1	24h_half_life (r=0.5)
7	18.851570	0.156119	569.053942	0.1	24h_half_life (r=0.5)
8	18.925788	0.156557	562.894324	0.1	24h_half_life (r=0.5)
9	18.962897	0.156778	557.318071	0.1	24h_half_life (r=0.5)

Note: This table reports the deterministic PK→PD mapping without suppression overlays. The full day-by-day grid (132 rows) is provided in the referenced CSV for reproducibility.

Table 10: Toy suppression band grid by α (`lgd_toy_pkpd_suppression_bands_by_alpha.csv`).

Scenario	Dose (mg/day)	Day	$p_{5\%}$	$p_{50\%}$	$p_{95\%}$	min	max	n_α
24h_half_life (r=0.5)	0.1	0	0.0	0.0	0.0	0.0	0.0	5
24h_half_life (r=0.5)	0.1	1	0.7651564323499429	0.9803822800416514	1.4569979894708351	0.7458009379054966	1.5205345508232435	5
24h_half_life (r=0.5)	0.1	2	1.7887065646446618	2.26265718751687	3.280079421964549	1.7457983701239552	3.414286061804264	5
24h_half_life (r=0.5)	0.1	3	2.9195233935214607	3.6207652992407888	5.085160683127006	2.8490987453203257	5.292207663506783	5
24h_half_life (r=0.5)	0.1	4	4.134086829622172	4.964016631344749	6.81095296938074	4.025246065205068	7.108600005018937	5
24h_half_life (r=0.5)	0.1	5	5.394286722757567	6.240109219292719	8.19608884267765	5.243975632598013	8.560711963676226	5
24h_half_life (r=0.5)	0.1	6	6.702498917985646	7.421972194864452	9.507186212429722	6.53213281440276	9.958078224823568	5
24h_half_life (r=0.5)	0.1	7	7.974612978197919	8.409141006585284	10.636350862046048	7.820597808999174	11.155172968387673	5
24h_half_life (r=0.5)	0.1	8	9.242333259467184	9.320410307434623	11.655200126152365	9.13709897696734	12.120346521094756	5
24h_half_life (r=0.5)	0.1	9	10.457972731480216	10.162200077063516	12.50736526566831	10.45532541555377	12.949845240165195	5
24h_half_life (r=0.5)	0.1	10	11.624789621571911	10.943501312998986	13.24665780222977	11.79294509217968	13.66813799393946	5
24h_half_life (r=0.5)	0.1	11	12.734547631308925	11.671020185459585	13.897782261940768	13.1014332371937	14.300372548000521	5

Note: The referenced CSV contains a full grid (132 rows) across days, doses, and scenarios; the table shows the initial segment for compactness. Percentiles are computed across the discrete α grid (size n_α) for each (scenario, dose, day).

Table 11: Monte Carlo suppression bands under lognormal α (`Monte Carlo lognormal alpha suppression bands.csv`).

Scenario	Dose (mg/day)	Day	n_{MC}	$p_{1\%}$	$p_{5\%}$	$p_{25\%}$	$p_{50\%}$	$p_{75\%}$	$p_{95\%}$	$p_{99\%}$
24h_half_life (r=0.5)	0.1	0	15000	0.0	0.0	0.0	0.0	0.0	0.0	0.0
24h_half_life (r=0.5)	0.1	1	15000	0.7219183233746546	0.7718444202300995	0.8784804837167486	0.981783545092242	1.1185418530977662	1.4039059343823863	1.6696756954766274
24h_half_life (r=0.5)	0.1	2	15000	1.692560017254941	1.803718917251718	2.039454892939583	2.265712571418074	2.562178215625663	3.169979220659247	3.7232801414541704
24h_half_life (r=0.5)	0.1	3	15000	2.770767077778423	2.9341411656018616	3.2805369764275034	3.6208614329347645	4.062202009101932	4.959661559811619	5.752398656828242
24h_half_life (r=0.5)	0.1	4	15000	3.9399693173661503	4.155475338700205	4.613975361008095	5.070810370372911	5.663367939437903	6.849201485333708	7.870823609197707
24h_half_life (r=0.5)	0.1	5	15000	5.160626270267284	5.432256509407877	6.003118227114236	6.580789484600671	7.322996417957286	8.79010144630708	10.03268839791075
24h_half_life (r=0.5)	0.1	6	15000	6.426369473682848	6.758744668337776	7.452756795467303	8.163064050680195	9.061362277953004	10.805336833832072	12.2758641113629
24h_half_life (r=0.5)	0.1	7	15000	7.689289115835886	8.079743059844468	8.893166662516705	9.732083246961935	10.78507782487408	12.791546795433633	14.479628411662347
24h_half_life (r=0.5)	0.1	8	15000	8.92927570571271	9.37285752390612	10.293350216971327	11.247152325923978	12.439595384317737	14.669642409826733	16.55170590621607
24h_half_life (r=0.5)	0.1	9	15000	10.131544462762074	10.62232538845439	11.64278744685874	12.702589949302017	14.02496828671505	16.468333602729269	18.538369819425255
24h_half_life (r=0.5)	0.1	10	15000	11.285695132181694	11.812075207778438	12.91094224347652	14.05164804450398	15.474942932157742	18.047776376002425	20.230635003670132
24h_half_life (r=0.5)	0.1	11	15000	12.386049546661095	12.943928314238364	14.107349778417742	15.318234626540709	16.823465301387	19.514173046381658	21.82554694249869

Note: The referenced CSV contains the full grid (132 rows) across days, doses, and scenarios; the table shows the initial segment for compactness. Percentiles summarize Monte Carlo draws under lognormal recovery α uncertainty.

Table 12: Level-2 suppression bands under α + PD draw uncertainty (`lgd_level2_suppression_bands_mc_alpha_pd.csv`).

Engine	Scenario	Dose (mg/day)	Day	n_{MC}	$p_{1\%}$	$p_{5\%}$	$p_{25\%}$	$p_{50\%}$	$p_{75\%}$	$p_{95\%}$	$p_{99\%}$
Level2+: PK+lag+PD (H dose-dependent, gamma=0.25)	24h_half_life (r=0.5)	0.1	0	3000	0.0	0.0	0.0	0.0	0.0	0.0	0.0
Level2+: PK+lag+PD (H dose-dependent, gamma=0.25)	24h_half_life (r=0.5)	0.1	1	3000	0.7754841466624262	0.8485822029336991	0.9920102951012595	1.1394304774271098	1.3339813181157569	1.7127636319251684	2.1012279391978866
Level2+: PK+lag+PD (H dose-dependent, gamma=0.25)	24h_half_life (r=0.5)	0.1	2	3000	1.8192045701628583	1.9758874747062524	2.291495019359631	2.6139346837790713	3.0191501148151712	3.804495329449773	4.569634288743703
Level2+: PK+lag+PD (H dose-dependent, gamma=0.25)	24h_half_life (r=0.5)	0.1	3	3000	2.9498013909352674	3.1767443258018353	3.6265727813001575	4.084951366289109	4.662911690802531	5.783405021334735	6.85987286814789
Level2+: PK+lag+PD (H dose-dependent, gamma=0.25)	24h_half_life (r=0.5)	0.1	4	3000	4.152117482199534	4.439534050751119	5.003245878917448	5.577459531963439	6.304745392712532	7.723501832682232	9.08030251502433
Level2+: PK+lag+PD (H dose-dependent, gamma=0.25)	24h_half_life (r=0.5)	0.1	5	3000	5.38690790478350 85	5.734927733354918	6.422634383520605	7.122814302050928	8.019866461735307	9.792639504688411	11.485818840232262
Level2+: PK+lag+PD (H dose-dependent, gamma=0.25)	24h_half_life (r=0.5)	0.1	6	3000	6.639411126316701	7.051921295138636	7.856826769151719	8.675940560846659	9.727226826155312	11.846166894938562	13.870831012640673
Level2+: PK+lag+PD (H dose-dependent, gamma=0.25)	24h_half_life (r=0.5)	0.1	7	3000	7.888900921011092	8.367284530342249	9.307382206985246	10.269099653744422	11.498508157507544	13.93673984368034	16.251200459687594
Level2+: PK+lag+PD (H dose-dependent, gamma=0.25)	24h_half_life (r=0.5)	0.1	8	3000	9.116892486300855	9.660896046194546	10.733944823806733	11.837747329947202	13.24457129481086	15.985825261583495	18.578990587642704
Level2+: PK+lag+PD (H dose-dependent, gamma=0.25)	24h_half_life (r=0.5)	0.1	9	3000	10.30823973389024	10.916187753481934	12.112964829335205 3	13.349161060963 46	14.923384650239619	17.907548559116474	20.719960683827 71
Level2+: PK+lag+PD (H dose-dependent, gamma=0.25)	24h_half_life (r=0.5)	0.1	10	3000	11.449495532838362	12.120460127382755	13.438903590246212	14.808681380180357	16.54931400434158	19.763021165368017	22.767368763649 72
Level2+: PK+lag+PD (H dose-dependent, gamma=0.25)	24h_half_life (r=0.5)	0.1	11	3000	12.531082183793285	13.263285369582731	14.704917924153952	16.208933981828918	18.117799287262 67	21.542070305988 44	24.711233737210457

Note: The referenced CSV contains the full grid (264 rows) across days, doses, scenarios, and engine configurations; the table shows the initial segment for compactness. Percentiles summarize Monte Carlo suppression bands under joint α uncertainty and PD-draw uncertainty.

Table 13: α-sensitivity diagnostics: β re-fit that preserves the day-21 endpoint (`Alpha-sensitivity__beta_re-fit__hits_TT21_for_each_alpha_2.csv`).

Scenario	Dose (mg/day)	H (days)	α (day^{-1})	β (re-fit)	TT_{21} target	TT_{21} check
24h_half_life (r=0.5)	0.1	5.0	0.12944943670387588	0.1638517671170262	506.0	505.99999999999994
24h_half_life (r=0.5)	0.1	7.0	0.09427633573609329	0.12961848432678957	506.0	506.0
24h_half_life (r=0.5)	0.1	10.0	0.06696700846319259	0.10564532647289751	506.0	505.99999999999994
24h_half_life (r=0.5)	0.1	14.0	0.04830484698938042	0.09079567534939317	506.0	506.0000000000001
24h_half_life (r=0.5)	0.1	20.0	0.0340636710751544	0.08036700088609561	506.0	505.99999999999994
24h_half_life (r=0.5)	0.3	5.0	0.12944943670387588	0.09544012322829648	436.0	436.0
24h_half_life (r=0.5)	0.3	7.0	0.09427633573609329	0.08509668183827314	436.0	436.0
24h_half_life (r=0.5)	0.3	10.0	0.06696700846319259	0.07774031570708127	436.0	435.99999999999994
24h_half_life (r=0.5)	0.3	14.0	0.04830484698938042	0.07249289899339496	436.0	436.0
24h_half_life (r=0.5)	0.3	20.0	0.0340636710751544	0.06878239569224927	436.0	436.0
24h_half_life (r=0.5)	1.0	5.0	0.12944943670387588	0.09784971580303582	340.0	340.0000000000001
24h_half_life (r=0.5)	1.0	7.0	0.09427633573609329	0.09445784449039219	340.0	339.99999999999994
24h_half_life (r=0.5)	1.0	10.0	0.06696700846319259	0.09205337573828762	340.0	340.0
24h_half_life (r=0.5)	1.0	14.0	0.04830484698938042	0.09032259750415961	340.0	340.0000000000001
24h_half_life (r=0.5)	1.0	20.0	0.0340636710751544	0.08909680486029955	340.0	340.0
36h_half_life (r=0.63)	0.1	5.0	0.12944943670387588	0.16436782693245218	506.0	506.0
36h_half_life (r=0.63)	0.1	7.0	0.09427633573609329	0.12995596177497862	506.0	505.99999999999994
36h_half_life (r=0.63)	0.1	10.0	0.06696700846319259	0.1072797359984482	506.0	505.99999999999994
36h_half_life (r=0.63)	0.1	14.0	0.04830484698938042	0.09424782976087288	506.0	505.99999999999994
36h_half_life (r=0.63)	0.1	20.0	0.0340636710751544	0.08583873793965974	506.0	506.0000000000001
36h_half_life (r=0.63)	0.3	5.0	0.12944943670387588	0.09579402893642943	436.0	436.0
36h_half_life (r=0.63)	0.3	7.0	0.09427633573609329	0.08532343994683944	436.0	436.0
36h_half_life (r=0.63)	0.3	10.0	0.06696700846319259	0.07845934064043981	436.0	436.0000000000001
36h_half_life (r=0.63)	0.3	14.0	0.04830484698938042	0.07378345652908075	436.0	436.0
36h_half_life (r=0.63)	0.3	20.0	0.0340636710751544	0.07078351474252205	436.0	436.0
36h_half_life (r=0.63)	1.0	5.0	0.12944943670387588	0.09793254330901303	340.0	340.0
36h_half_life (r=0.63)	1.0	7.0	0.09427633573609329	0.09449053751485948	340.0	340.0
36h_half_life (r=0.63)	1.0	10.0	0.06696700846319259	0.09250494492919074	340.0	340.0000000000001
36h_half_life (r=0.63)	1.0	14.0	0.04830484698938042	0.09089224278016836	340.0	340.0
36h_half_life (r=0.63)	1.0	20.0	0.0340636710751544	0.08985368696795416	340.0	340.0

Table 14: Lag-model fit summary showing exact day-21 anchoring (`lag_model_fit_summary__matches_day-21_TT_.csv`).

Scenario	Dose (mg/day)	AUC_{21}	Observed TT_{21}	Simulated TT_{21}	α (day^{-1})	β (fitted)
24h_half_life (r=0.5)	0.1	19.0	506.0	505.99999999999994	0.06696700846319259	0.10564532647289751
24h_half_life (r=0.5)	0.3	85.0	436.0	435.99999999999994	0.06696700846319259	0.07774031570708127
24h_half_life (r=0.5)	1.0	238.0	340.0	340.0	0.06696700846319259	0.09205337573828762
36h_half_life (r=0.63)	0.1	19.0	506.0	505.99999999999994	0.06696700846319259	0.1072797359984482
36h_half_life (r=0.63)	0.3	85.0	436.0	436.0000000000001	0.06696700846319259	0.07845934064043981
36h_half_life (r=0.63)	1.0	238.0	340.0	340.0000000000001	0.06696700846319259	0.09250494492919074

Table 15: Full posterior-ish PD draw list used for PD uncertainty propagation (`lgd_level2_pd_draws_posteriorish.csv`).

Draw #	Emax	EC50
1	0.5007658716171357	44.46988252823651
2	0.5169504764882505	55.95064937596627
3	0.4844195211710093	28.032835329904405
4	0.5337729995147982	48.761358949979495
5	0.5460482097000185	52.74459681871729
6	0.5496757694366949	55.78771183060093
7	0.5102946596767099	39.69529664466903
8	0.5547480014311013	43.63113736553106
9	0.5509909104418895	45.90237070425788
10	0.489292763165237	39.24920502472373
11	0.519709056978608	39.00020735224828
12	0.5258835716395977	50.25368270672351
13	0.5247864950688438	62.695642646965676
14	0.5121204605196767	48.83751607946926
15	0.547457656412786	41.301043530663404
16	0.5414694325549982	40.22567800681411
17	0.4684026160638655	40.37407461221498
18	0.5307563261684539	56.54376058062968
19	0.5358815652536368	43.87650494972602
20	0.5290049635378058	29.089602801727864
21	0.5558310469458124	38.0098116889972
22	0.4937806956662294	35.421125276818446
23	0.5374686310883946	45.8280233569753
24	0.5002146792074948	34.60016249896934
25	0.5458056422929379	42.516959302016646
26	0.519514414380718	41.19677439954824
27	0.5410851429591261	39.556816312434055
28	0.5222163988354088	36.31788959521265
29	0.5451537809784169	32.64648224787952
30	0.5009084946427273	44.89483238911098
31	0.4792947175026528	54.608094269729085
32	0.5220254773896099	57.570941866349194
33	0.5530199726515095	31.065417785239085
34	0.5446040330389768	61.38493252266271
35	0.4992298301956408	37.97390215544555
36	0.534823876661715	36.81762099781017
37	0.5074621526402414	46.81741667674302
38	0.5122268514100967	54.16552728896039
39	0.5023806719660712	54.87592447078392
40	0.4684979704562	32.076138471699764

Note: The CSV contains 2000 draws; only the first 40 are shown here for compactness. The full list is the reproducibility artifact referenced in the caption.

C Mathematical Derivations

First-Order Elimination and Steady-State Accumulation:

Assume first-order elimination with rate constant

$$k = \frac{\ln 2}{t_{1/2}}, \tag{12}$$

where $t_{1/2}$ denotes the elimination half-life. Between doses, plasma concentration decays exponentially:

$$C(t) = C_0 e^{-kt}. \tag{13}$$

For a fixed dosing interval $\tau = 24$ hours, the fraction of drug remaining at the next dose is

$$r = e^{-k\tau} = 2^{-\tau/t_{1/2}}. \tag{14}$$

Let A_n denote the amount immediately after the nth daily dose of magnitude D. The accumulation dynamics satisfy the linear recurrence

$$A_n = rA_{n-1} + D, \qquad A_1 = D. \tag{15}$$

Solving this recursion yields

$$A_n = D\sum_{j=0}^{n-1} r^j = D\frac{1-r^n}{1-r}. \tag{16}$$

As $n \to \infty$, the steady-state amount converges geometrically to

$$A_\infty = \frac{D}{1-r}, \tag{17}$$

which defines the standard accumulation factor

$$R = \frac{1}{1-r}. \tag{18}$$

Saturating Pharmacodynamic Response:

Exposure is mapped to a fractional suppression signal using a standard saturating response:

$$y(x) = \frac{E_{\max} x}{EC_{50} + x}. \tag{19}$$

This form captures diminishing marginal suppression at higher exposure levels and avoids the linear dose–response assumption. The function is monotone, bounded, and analytically tractable.

Exposure Scaling via AUC Anchoring:

Rather than modeling instantaneous concentration, exposure is defined as the area under the concentration–time curve over each dosing interval:

$$\mathrm{AUC}_{0-24} = \int_0^{24} C(t)\,dt. \tag{20}$$

Under first-order elimination, cumulative exposure increases monotonically toward steady state with the same geometric structure as accumulation. Let x_t denote relative exposure on day t. Anchoring to the clinically reported day-21 exposure x_{21} yields

$$x_t = x_{21}\,\frac{1-r^t}{1-r^{21}}, \tag{21}$$

where $r = e^{-24k}$.

This construction ensures that modeled exposure:

1. Is consistent with first-order pharmacokinetics,
2. Preserves monotonic accumulation,
3. Exactly reproduces the observed clinical endpoint at day 21.

Lagged Testosterone Dynamics:

Testosterone suppression is governed by an indirect-response model incorporating delayed feedback:

$$TT_{t+1} = TT_t + \alpha\,(TT_{\text{baseline}} - TT_t) - \beta\,y(x_t)\,TT_{\text{baseline}}. \tag{22}$$

Here:

- α controls recovery toward baseline,
- β scales exposure-driven suppression,
- $y(x_t)$ is the instantaneous suppression signal.

This discrete-time formulation approximates a continuous-time linear recovery with exposure-driven forcing while remaining numerically stable and interpretable.

Recovery Half-Life Parameterization:

To reflect inter-individual variability, recovery is parameterized via a half-life H:

$$\alpha = 1 - e^{-\ln 2/H}. \tag{23}$$

Sampling H from a lognormal distribution ensures positivity and accommodates right-skewed recovery times. For each draw of α, the suppression coefficient β is solved such that

$$TT_{21}^{\text{model}} = TT_{21}^{\text{clinical}}, \tag{24}$$

enforcing exact endpoint anchoring.

D Updated! (For Reddit)

Goal 1 — Endpoint Suppression, Velocity, and Implied Exposure

To compare heterogeneous anecdotal reports under a unified framework, we decompose the analysis into three steps: (i) endpoint-based suppression, (ii) time-normalized suppression velocity, and (iii) inversion to an implied exposure band under a pharmacodynamic (PD) model class. This approach prioritizes robustness to sparse, irregular, and self-reported data while maintaining explicit assumptions.

1A. Observed suppression fraction (endpoint-based). For each case, we compute the observed suppression fraction

$$y_{\text{obs}} \;=\; \frac{TT_{\text{pre}} - TT_{\text{post}}}{TT_{\text{pre}}}, \tag{25}$$

and report the corresponding percentage suppression as $100\, y_{\text{obs}}$. This quantity represents the minimal, assumption-free summary of the endpoint change and answers the question: *what happened between measurements.*

1B. Suppression velocity (time-normalized). Because anecdotal cycles vary widely in duration, we additionally compute a time-normalized suppression velocity,

$$v \;=\; \frac{100\, y_{\text{obs}}}{\Delta t_{\text{weeks}}}, \tag{26}$$

where Δt_{weeks} is the elapsed time between measurements in weeks. This metric highlights short, high-intensity exposures that may appear moderate when viewed only through endpoints.

1C. Inversion to implied exposure (model lens). To interpret observed suppression in exposure space, we invert a pharmacodynamic model anchored to clinical data. Under a standard Emax formulation,

$$y(x) \;=\; E_{\max}\, \frac{x}{EC_{50} + x}, \tag{27}$$

where x denotes an exposure proxy (here, AUC-like), $E_{\max}$ is the maximal achievable suppression, and EC_{50} is the half-maximal exposure.

Uncertainty in $(E_{\max}, EC_{50})$ is represented via Monte Carlo draws constrained to reproduce clinical day-21 suppression anchors. For a given observation time t^*, we define the implied exposure set

$$\mathcal{X}(t^*) \;=\; \big\{\, x \;:\; y(t^*; x) \in [q_5(t^*),\, q_{95}(t^*)] \,\big\}, \tag{28}$$

where q_5 and q_{95} denote the 5th and 95th percentiles of the model envelope. If $y_{\text{obs}} \geq E_{\max}$ for all draws, no inversion exists under this model class; such cases are flagged rather than forced to fit.

Model class expansion: Hill (sigmoid) extension.

The fixed-slope Emax model implicitly conflates response steepness with maximal suppression. To separate these effects, we expand the PD class by introducing a Hill coefficient n,

$$y(x) \;=\; E_{\max}\, \frac{x^n}{EC_{50}^n + x^n}. \tag{29}$$

This formulation contains the standard Emax model as the special case $n = 1$ but permits threshold-like behavior ($n > 1$), allowing high suppression at large exposure without requiring implausible values of $E_{\max}$.

Importantly, the Hill extension does not overwrite the original model: moderate-suppression cases remain largely unchanged, while extreme endpoints become admissible only under steep-response assumptions. This explicitly encodes heterogeneity rather than obscuring it.

Interpretation for anecdotal data. Because self-reported cycles are sparse, heterogeneous, and often lack intermediate measurements, inversion is used here as a *model lens*, not a dose estimator. Cases that invert cleanly lie within the clinical suppression envelope; cases that invert only under steep Hill slopes highlight potential biological sensitivity, timing mismatch, or unmodeled confounding. Cases that fail inversion under conservative assumptions are retained and flagged, not discarded. *Basically, this structure allows anecdotal observations to be compared coherently while preserving uncertainty and avoiding over-interpretation.*

Goal 1 — Results and empirical patterns

Applying the Goal 1 framework to the collected anecdotal dataset yields several stable empirical patterns that are robust across model variants and exposure normalizations. These findings are descriptive rather than predictive and are intended to clarify how heterogeneous reports relate to clinically anchored suppression dynamics.

Endpoint suppression versus nominal dose. Observed endpoint suppression spans a wide range across cases, including substantial suppression at nominally low daily doses and overlapping endpoints across markedly different regimens. No simple monotonic relationship between stated daily dose and endpoint suppression is evident. This reinforces the motivation for treating nominal dose as an unreliable proxy for endocrine impact in anecdotal settings.

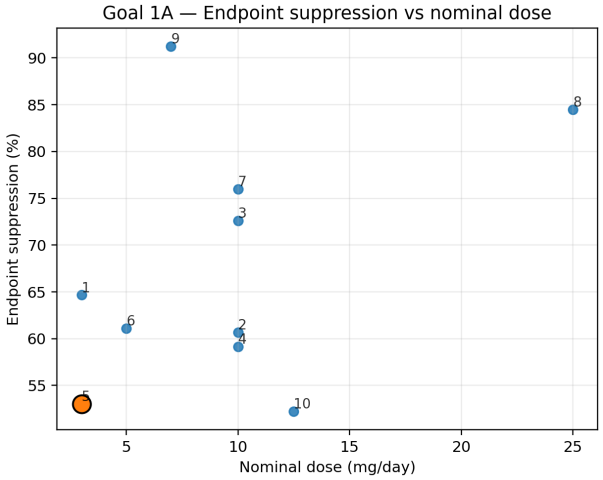

Figure 8: Endpoint suppression versus nominal daily dose across anecdotal cases.

Figure 8 visualizes endpoint suppression fraction against reported daily dose. The dispersion highlights that similar suppression endpoints can arise from very different dosing patterns, durations, and individual responses.

Time-normalized suppression velocity isolates short-cycle effects. When suppression is normalized by elapsed time, short-duration cycles with large endocrine disruption emerge clearly as high-velocity outliers. These cases may appear unremarkable when viewed solely through endpoints but dominate when viewed through suppression velocity.

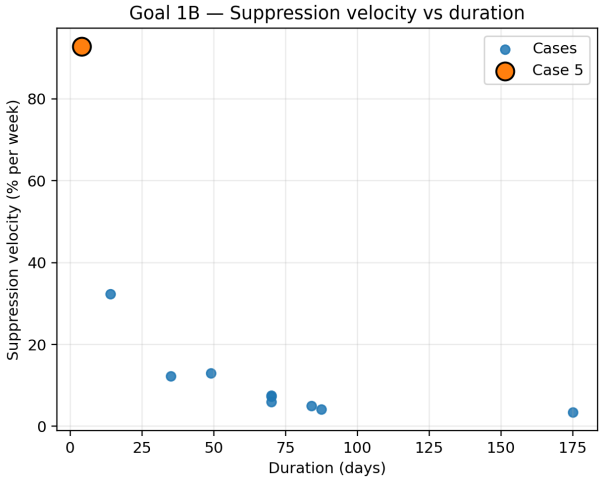

Figure 9: Suppression velocity versus cycle duration across anecdotal cases.

Figure 9 plots suppression velocity against cycle duration. The separation of short, high-intensity cycles from longer regimens demonstrates that duration is a critical confounder in anecdotal comparisons and cannot be ignored.

Implied exposure bands under PD inversion. Inversion to implied exposure space reveals that all cases admitting a solution under the Hill-extended model imply exposure levels exceeding the clinical 1 mg/day reference regime. Moderate-suppression cases invert under both fixed-slope and Hill formulations with comparable median implied exposures, indicating stability in the center of the distribution.

In contrast, extreme-suppression cases that failed inversion under the fixed-slope Emax model become admissible only under steep Hill responses. For these cases, the implied exposure intervals are wide, explicitly reflecting uncertainty rather than forcing a precise estimate.

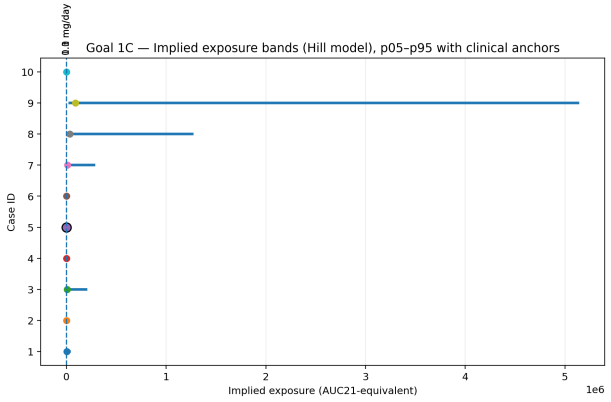

Figure 10: Implied exposure bands (Hill model) with clinical reference anchors.

Figure 10 summarizes the implied exposure intervals for all cases, alongside clinical reference anchors. Cases with no admissible inversion under conservative assumptions are retained and flagged rather than excluded.

Interpretive synthesis. Taken together, the Goal 1 results support three key conclusions:

1. Nominal daily dose alone is an insufficient descriptor of endocrine impact in anecdotal data.

2. Suppression velocity provides essential context for identifying short, high-intensity exposures that are otherwise obscured.

3. Pharmacodynamic inversion, particularly under a Hill-extended model class, allows heterogeneous endpoints to be compared against a shared clinical reference while preserving uncertainty and heterogeneity.

Crucially, the Hill extension repairs incompatibilities at the extremes without distorting the behavior of typical cases. This indicates that the observed variability arises from response heterogeneity rather than from failure of the clinical anchors themselves.

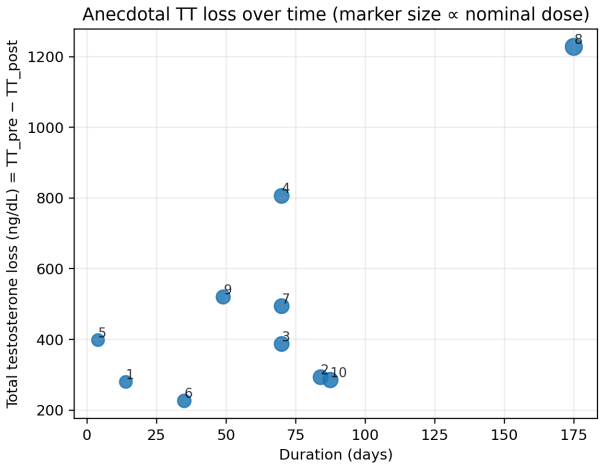

Special Case 1: Mid-cycle trajectory check under end-point anchoring

We treat the mid-cycle datapoint as a *trajectory-shape diagnostic*, not a fitted target. The objective is to assess whether the suppression dynamics implied by the model are compatible with the observed time course, conditional on the same final suppression.

For each Monte Carlo draw, we proceed as follows:

1. Fix the pharmacokinetic accumulation shape via a decay ratio $r \in \{0.5, 0.63\}$.
2. Sample pharmacodynamic parameters $(E_{\max}, EC_{50}, n)$ from the Hill-extended PD draw set.
3. Sample recovery dynamics via α, with $H \sim$ lognormal and $\alpha = 1 - e^{-\ln 2/H}$.
4. Construct the exposure trajectory x_t under the toy accumulation model.
5. *Re-fit* the suppression gain β so that the model exactly matches the observed endpoint:

$$TT(84) = TT_{\text{end}}^{\text{obs}}.$$

Because the state equation is linear in β for fixed $(\alpha, E_{\max}, EC_{50}, n)$, this step uniquely determines β for each draw. Consequently, every simulated trajectory is constrained to terminate at the observed final testosterone level, removing endpoint ambiguity entirely.

Conditional midpoint distribution. After anchoring the endpoint, we read off the implied midpoint testosterone level at $t_{\text{mid}} = 42$ days. Each Monte Carlo draw therefore contributes one realization of

$$TT_{\text{mid}}^{\text{pred}} \mid \left(TT_{\text{end}} = TT_{\text{end}}^{\text{obs}}\right),$$

yielding a conditional distribution for the midpoint given the same final suppression. The resulting histograms thus answer the question:

> *"Given that this individual ended at TT_{end}, where should they have been halfway through if suppression followed the model-implied dynamics?"*

For special_1 (10 mg/day for 84 days; $TT_{\text{pre}} = 483$, $TT_{\text{mid}} = 286$, $TT_{\text{end}} = 190$ ng/dL), the predicted midpoint distributions are:

$$\text{24h scenario } (r = 0.5):$$

$$[p05, p50, p95] = [192.38,\ 212.42,\ 260.84] \text{ ng/dL},$$

$$\text{36h scenario } (r = 0.63):$$

$$[p05, p50, p95] = [192.42,\ 212.58,\ 261.19] \text{ ng/dL}.$$

In both cases, the observed midpoint $TT_{\text{mid}}^{\text{obs}} = 286$ ng/dL lies above the 95th percentile, indicating that mid-cycle suppression is systematically *weaker* than the model predicts, conditional on the same final suppression.

Interpreting early vs. late suppression. Although the cycle is naturally divided into two equal 42-day segments, no explicit "first-half vs. second-half" averaging is performed. Time enters only through the exposure trajectory $x(t)$ and the daily state update:

$$TT_{t+1} = TT_t + \alpha\,(TT_0 - TT_t) - \beta\, y(x_t)\, TT_0,$$

$$y(x) = \frac{E_{\max} x^n}{EC_{50}^n + x^n}.$$

If suppression were approximately symmetric or accumulation-driven, roughly half of the total suppression would be realized by t_{mid}. Conversely, early-heavy suppression would imply a *lower* TT_{mid}, while late-accelerating suppression would imply a *higher* TT_{mid}.

Here the observed midpoint lies substantially above the conditional prediction band, implying that—given the same final outcome—*less* suppression occurred during weeks 1–6 and *more* suppression was deferred to weeks 7–12 than the model expects. This diagnoses late acceleration without explicitly segmenting the timeline.

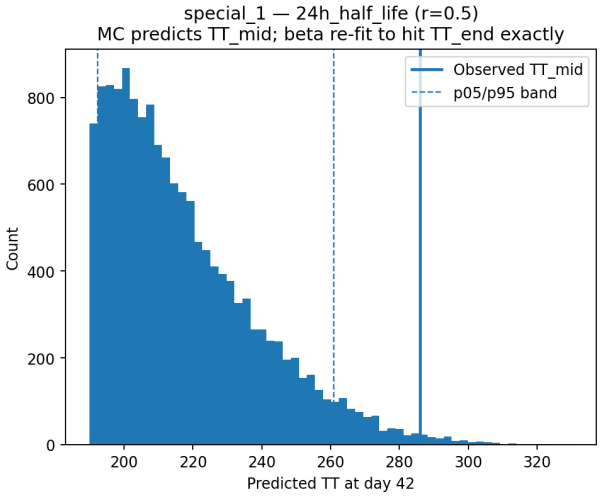

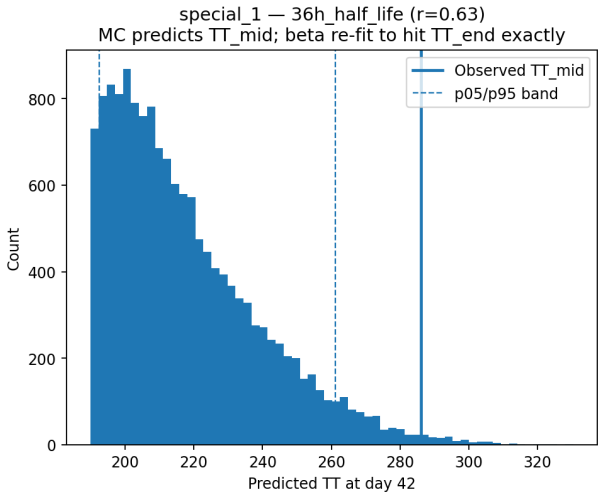

Why endpoint anchoring is essential. Had we instead fitted both the midpoint and endpoint independently, we would double the number of fitted targets, inflate degrees of freedom, and lose identifiability. By fitting only the endpoint and testing an interior point, we perform a shape validation rather than a refit. This is the statistically correct use of sparse mid-cycle data, particularly in anecdotal settings where measurement noise and protocol heterogeneity are unavoidable.

The persistence of the midpoint mismatch across PK scenarios further indicates that the discrepancy is not driven primarily by half-life tuning, but reflects trajectory-shape dynamics beyond simple accumulation lag.

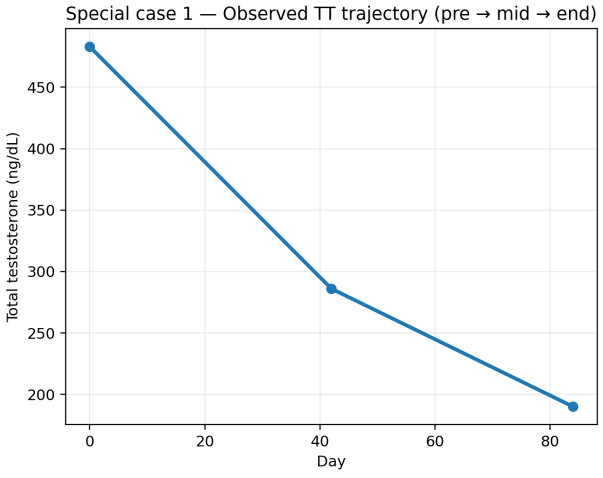

Special Case 2: Schedule-aware effective dose versus time-averaged dose

This analysis isolates a distinct but related question: how should a non-constant dosing schedule be summarized as a single "effective dose" under a nonlinear dose–response relationship? The goal is not to fit a pharmacokinetic or pharmacodynamic trajectory, but to test whether the commonly used *time-weighted average daily dose* is an adequate proxy for biologically relevant exposure when the dose–effect mapping is concave.

Observed suppression metrics. For special_2, suppression is computed endpoint-wise as

$$y_{\text{obs}} \equiv \frac{TT_{\text{pre}} - TT_{\text{post}}}{TT_{\text{pre}}},$$

with a time-normalized suppression velocity

$$v_{\text{supp}} \equiv \frac{100\, y_{\text{obs}}}{T/7} \ \%\ \text{per week},$$

where T is the total duration of the dosing schedule. These quantities provide descriptive context but are not used to infer schedule effects directly.

Time-weighted average dose. The standard scalar summary of a non-constant regimen is the time-weighted mean dose

$$\bar{d} \equiv \frac{\sum_i d_i\, \Delta t_i}{\sum_i \Delta t_i},$$

which treats dose as linearly additive across time. Under this definition, a short period of high dosing contributes proportionally to its duration, regardless of nonlinearities in the biological response.

Schedule-aware Emax-weighted effective dose. To account for nonlinear dose–response behavior, we instead summarize the schedule in *effect space*. Using a standard Emax mapping with Hill coefficient fixed to $n = 1$,

$$y(d) = \frac{E_{\max}\, d}{EC_{50} + d},$$

we compute the time-averaged pharmacodynamic drive

$$\bar{y} \equiv \frac{1}{T} \sum_{t=1}^{T} y(d(t)),$$

where $d(t)$ denotes the dose administered on day t. We then define a schedule-aware constant-dose equivalent d_{eff} by inverting the Emax function:

$$d_{\text{eff}} \equiv y^{-1}(\bar{y}) = \frac{EC_{50}\, \bar{y}}{E_{\max} - \bar{y}}, \qquad 0 < \bar{y} < E_{\max}.$$

This quantity answers the question: *what constant daily dose would generate the same average pharmacodynamic effect as the observed schedule?*

Interpretation. Because $y(d)$ is concave in d, high-dose days contribute disproportionately to $\bar{y}$ relative to their contribution to $\bar{d}$. As a result, schedules with brief high-dose phases generally satisfy

$$d_{\text{eff}} > \bar{d},$$

even when total milligram exposure is fixed. We report the ratio

$$\frac{d_{\text{eff}}}{\bar{d}}$$

as a compact measure of schedule amplification beyond linear averaging.

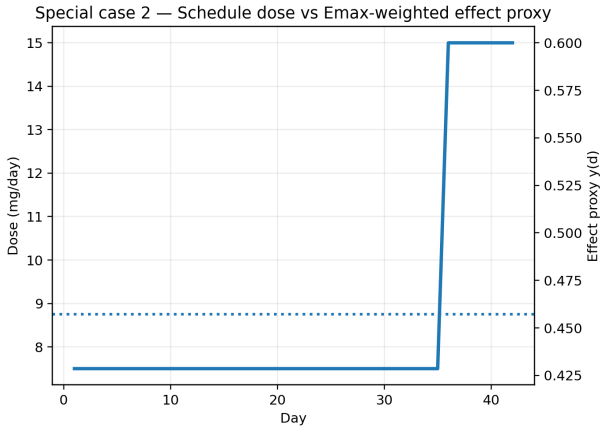

Conceptual implication. This analysis demonstrates that dose averaging is not equivalent to exposure averaging under nonlinear pharmacodynamics. Collapsing non-constant regimens into a single mean dose can systematically understate biologically relevant exposure when suppression is driven by a concave dose–effect relationship. Importantly, this conclusion follows directly from the shape of the response function and does not depend on fitting testosterone trajectories or invoking additional model degrees of freedom.

Relation to trajectory-based analyses. Whereas Goal 2 diagnoses imbalance between early and late suppression via trajectory shape under endpoint anchoring, Special Case 2 shows that even before dynamic modeling, the scalar representation of dose already encodes schedule-dependent information. Together, these results indicate that both exposure summarization and suppression timing must be treated carefully when interpreting heterogeneous anecdotal outcomes.

Reminder: Dose Labels, Accumulation, and Exposure

A critical clarification concerns the relationship between reported dose labels and the quantities that actually drive suppression in the model.

Conceptual distinction. The suppression model developed in Goal 1 does *not* operate on nominal daily dose (e.g., "3 mg/day"). Instead, it operates on *effective exposure*, which already incorporates drug accumulation arising from long elimination half-life and repeated dosing. In this sense,

- a label such as "3 mg/day" represents a *dosing instruction*, whereas
- the biological system responds to a substantially higher *steady-state exposure*, typically on the order of $\sim$ 6–8 mg equivalent depending on half-life (24–36 h).

No mathematical inconsistency is present in the analysis; what is required is simply an explicit interpretive bridge between dose labels and exposure-driven effects.

Accumulation and exposure (PK layer). Under first-order elimination with elimination rate constant k and dosing interval τ, repeated dosing produces an accumulation factor

$$R \;=\; \frac{1}{1-e^{-k\tau}}. \tag{30}$$

For LGD-4033, plausible half-lives imply

$$\text{24 h half-life: } R \approx 2.0, \qquad \text{36 h half-life: } R \approx 2.7.$$

Accordingly, a reported daily dose D corresponds to an effective steady-state amount approximately

$$\text{effective exposure} \;\approx\; R \cdot D.$$

This accumulation logic is not an auxiliary adjustment but is already embedded in the analysis through (i) construction of AUC-like exposure proxies, (ii) anchoring to clinical day-21 suppression data, and (iii) inversion to implied exposure bands. These steps are developed explicitly in Sections 3.1–3.3 and 4.2–4.3.

Suppression model acts on exposure, not dose. The pharmacodynamic mapping throughout Goal 1 is

$$x_t \;\longrightarrow\; y(x_t), \tag{31}$$

where x_t denotes exposure (AUC-like), not raw dose. Thus, when figures refer to "3 mg/day" or similar labels, these serve only as identifiers of the dosing regimen rather than as the variables governing suppression.

The exposure trajectory itself arises from accumulated dosing,

$$x_t \;\propto\; \sum_{i=1}^{t} D\, e^{-k(t-i)}, \tag{32}$$

which captures both accumulation and decay across time. It is this quantity—not D directly—that enters the Emax or Hill suppression functions used in inversion and velocity analyses.

Implications for interpretation. Dose labels are therefore retained for interpretability and consistency with anecdotal reporting, while all suppression, velocity, and implied exposure results are driven by accumulated exposure. This distinction explains why apparently "low-dose" regimens can produce substantial suppression and reinforces the central theme of this work: *dosage is not equivalent to exposure.*